

A depositional model for deep-lacustrine, partially confined, turbidite fans: early Cretaceous, North Falkland Basin

Thomas J.H. Dodd*¹, Dave J. McCarthy¹ and Philip C. Richards

¹British Geological Survey, the Lyell Centre, Research Avenue South, Edinburgh, EH14 4AP, United Kingdom, tdodd@bgs.ac.uk

ABSTRACT

This paper presents a model of facies distribution within a set of early Cretaceous, deep-lacustrine, partially confined turbidite fans (Sea Lion Fan, Sea Lion North Fan, Otter Fan) in the North Falkland Basin, South Atlantic. As a whole, ancient deep-lacustrine turbidite systems are underrepresented in the literature when compared with those documented in marine basins. Lacustrine turbidite systems can form extensive, good quality hydrocarbon reservoirs, making the understanding of such systems crucial to exploration within lacustrine basins. An integrated analysis of seismic cross sections, seismic amplitude extraction maps, and 455 m of core has enabled the identification of a series of turbidite fans. The deposits of these fans have been separated into lobe axis, lobe fringe and lobe distal fringe settings. Seismic architectures, observed in the seismic amplitude extraction maps, are interpreted to represent geologically associated heterogeneities, including: feeder systems, terminal mouth lobes, flow deflection, sinuous lobe axis deposits, flow constriction and stranded lobe fringe areas. When found in combination, these architectures suggest “partial confinement” of a system, something that appears to be a key feature in the lacustrine turbidite setting of the North Falkland Basin. Partial confinement of a system occurs when positionally generated topography controls the flow-pathway and deposition of subsequent turbidite fan deposits. The term “partial confinement” provides a term for categorising a system whose depositional boundaries are unconfined by the margins of the basin, yet exhibit evidence of internal confinement, primarily controlled by depositional topography. Understanding the controls that dictate partial confinement; and the resultant distribution of sand-prone facies within deep-lacustrine turbidite fans, is important, particularly considering their recent rise as hydrocarbon reservoirs in rift and failed-rift settings.

Keywords: Turbidites, North Falkland Basin, Sea Lion Fan, Partial Confinement, Hybrid Event Bed, Deep-Lacustrine.

INTRODUCTION

There is a significant body of published research on marine turbidite systems that form a large proportion of the world's major hydrocarbon reservoirs (Fugitt et al., 2000; Hempton et al., 2005; Mayall et al., 2006; Saller et al., 2008; Shanmugam et al., 2009). Despite there being a reasonable amount of published literature on modern-day lakes such as Lake Malawi, Africa (Crossley, 1984; Scholz et al., 1990; Lyons et al., 2011) and Lake Baikal, Russia (Nelson et al., 1999), and a proportion of literature addressing the ancient depositional environment as a whole (Buatois et al., 1996; Larsen and Smith, 1999; Saez and Cabrera, 2002; Moernaut et al., 2014), there is still relatively little in the way of published material describing the facies, facies architecture and development of ancient deep-lacustrine turbidites. Furthermore, there is a scarcity of literature that focuses on comparing and contrasting lacustrine systems and their marine counterparts.

Deep-lacustrine turbidite systems, form important hydrocarbon reservoirs and trapping geometries in a number of basins worldwide, such as: the Suphan Buri Basin, Thailand (Ronghe and Surarat, 2002), the Songliao Basin, China (Zhi-qiang et al., 2010), the Bohai Bay Basin, China (Zhang, 2004; Li et al., 2014) and the pre-salt rift basins of West Africa (Jungslager, 1999; MacDonald et al., 2003). A good example comes from the Lucian Formation, offshore South Gabon, where extreme variations in thickness and reservoir heterogeneity occur as a result of confinement of high-density turbidites along fault-related lake-floor depressions (Smith, 1995). These few examples suggest that lacustrine turbidite fans can be particularly heterogeneous and therefore may offer a different set of challenges to model than compared with marine systems.

Level of confinement: partially confined turbidite systems

Fully confined turbidite systems are restricted by encircling topography and have been referred to as ponded systems (Winker, 1996) or confined or contained systems (Southern et al., 2015) and are discussed further in Smith (1995). Other examples of turbidite systems are affected by confining topography, but are not fully restricted by encircling basin topography (e.g. Lomas and Joseph, 2004). Confining topography can be formed by: lateral or downstream basin margins (Amy et al., 2004; Kane et al., 2010; Southern et al., 2014); structural features on the basin floor (Davis et al., 2009);

or depositionally generated topography on the basin floor (i.e. lobe compensation; Mutti and Normark 1987; Straub and Pyles, 2012).

The term “partial-confinement” is used here in the depositional model for the Sea Lion Fan and refers to a system whose broad depositional boundaries are not restricted by encircling topography, the down-stream limits are largely unconfined, but evidence exists for confinement of internal geometries (within the fan). Confinement of internal geometries is likely generated by depositional topography, which controlled the distribution of subsequent turbidite flows. High flow efficiencies, in particular high flow volumes, may have produced more elongate fan deposits (Al Ja’Aidi et al., 2004) and therefore elongated depositional topography. Ultimately, partial confinement may result in fan deposits with more laterally constrained facies belts compared with examples from unconfined systems (Shanmugam and Moiola, 1988; Covault and Romans, 2009). If partial confinement is restricted to deep lacustrine turbidite fans, it may reflect an important difference in the type, style and degree of confinement compared to deep-marine systems.

Deep-lacustrine turbidites form important target reservoirs within the North Falkland Basin (NFB; Richards et al., 2006). The Sea Lion Fan was drilled as an exploration target by Rockhopper Exploration in 2010 resulting in the discovery of the Sea Lion Field. The Sea Lion Fan (also referred to as the Sea Lion Complex or Sea Lion Main Complex) has since been studied by various authors, resulting in a number of publications that examine aspects of fan distribution and reservoir architecture (Bunt, 2015; Griffiths, 2015; MacAulay, 2015; Williams, 2015; Williams and Newbould, 2015). This paper presents an integrated subsurface study that utilises core, wireline logs, seismic cross sections and seismic amplitude extraction maps to examine the deep-lacustrine fans in the North Falkland Basin, with the aim of answering the following questions: (i) What is the style and character of deposition within deep-lacustrine fans? (ii) What is the role of partial confinement in controlling lacustrine systems? (iii) How may this impact hydrocarbon reservoir modelling and development? (iv) How might lacustrine fans differ from their marine counterparts? In answering these questions and drawing on the observations and learnings from the description of the Sea Lion Fan, this paper provides a model for deposition within deep-lacustrine, partially confined turbidite fans, in general.

GEOLOGICAL BACKGROUND

The Falkland Islands and territorial waters (Fig. 1) are located around 300 km to the south-east of South America. The islands are surrounded by five Mesozoic-aged offshore basins: the South Falkland, Fitzroy, Volunteer, Malvinas and the North Falkland Basin (NFB). The NFB is a failed rift system (Richards et al., 1996a and 1996b), comprising a series of offset depocentres that are affected by two dominant structural trends: North-to-South oriented faulting is predominant in the northern NFB, whereas north-west to south-east oriented faults dominate the southern NFB. This study focuses on the northern portion of the NFB.

The northern extent of the basin has a half-graben geometry (Fig. 2), with major faults on the eastern margin that influenced deposition (Richards et al., 1996a and 1996b; Richards and Fannin, 1997; Richards and Hillier, 2000a; Lohr and Underhill, 2015). From the most-northerly limit to the southern edge, the entire NFB is approximately 250 km long and 100 km wide (from west to east). Rifting is likely to have initiated in the very latest Jurassic or early Cretaceous, with the NFB forming as a failed-rift arm associated with the opening of the South Atlantic (Richards et al., 1996). This rifting phase was then followed by a subsequent thermal sag phase that began in Berriasian-Valanginian times and continued under predominantly continental lacustrine deposition until Albian-Cenomanian times (Fig. 3), when the basin began to develop increasingly marine conditions (Richards et al., 1996a and 1996b; Richards and Fannin, 1997; Richards and Hillier, 2000a).

Up to 1,150 m of late Jurassic to early Cretaceous lacustrine claystones were deposited during the syn-rift and earliest post-rift stages of basin development (Richards and Hillier, 2000b). The thickest, most laterally extensive of these claystones were deposited during the early post-rift phase in Berriasian to early Aptian times (Fig. 3). These lacustrine claystones are organic-rich (up to 7.5% total organic content) and form the principal source rock for discovered hydrocarbons to date (Richards and Hillier, 2000a; 2000b). The early post-rift phase was dominated, at least in the northernmost part of the basin, by the southwards, axial progradation of a lacustrine deltaic system. The progradation of the deltaic units occurred contemporaneously with the deposition of easterly derived, slope apron fans, resulting in a complex inter-fingering of the systems within the basin centre. Five separate

phases of delta progradation and retreat or hiatus have been identified, additionally several lowstand phases have been mapped as regionally significant unconformities within the basin (Richards and Hillier, 2000a). The base of tectono-stratigraphic unit LC3 (Figs 2 & 3) represents one of these deltaic lowstand-associated unconformities. The LC3 unconformity represents the seismically defined surface onto which the partially confined, slope apron turbidite sediments of the Sea Lion Fan were deposited.

Several fans, including the Sea Lion Fan have been identified in the LC3 unit (Richards et al., 2006), which were subsequently imaged on a modern, more extensive 3D seismic dataset, and later drilled as part of Rockhopper's 2010 exploration campaign (MacAulay, 2015). Here we use the BGS genetic terminology that relates fans and lobes to the location of sediment entry points along the basin margin.

METHODS AND DATASETS

Over 4,500 km² of 3D seismic reflectivity data were acquired over the northern part of the NFB between 2007 and 2011. In 2012, three of the seismic surveys collected during this period were merged to form a single seismic volume. This study makes use of the merged, full-stack 3D volume, which has undergone Kirchhoff, pre-stack time migration and spectral broadening. The polarity of this data is zero phase European (SEG reversed polarity) and is displayed as such in all seismic cross sections in this paper.

Thirteen exploration/appraisal wells were drilled in the NFB in 2010-2011, nine of which penetrated the Sea Lion Fan. Seven of the nine wells were extensively cored in reservoir-prone sections, with over 455 m of conventional core recovered; all nine wells were logged with a comprehensive suite of wireline surveys undertaken. The 455 m of core has been logged at a scale of 1:10 cm to capture information on grain size, lithology and sedimentary structures. Cores have been sampled from the proximal, medial and distal deposits of the Sea Lion Fan, thereby providing sufficient geographical distribution of data.

Initial interpretations to build a depositional framework focussed on the identification of fans as imaged on seismic reflection profiles. Once the individual fans and lobes had been identified and their distributions mapped on seismic sections within the 3D

volume, a series of seismic reflection amplitude extraction maps were produced. The amplitude extractions were compiled by extracting average seismic amplitudes from a +/- 10 millisecond window above and below the mapped horizon. The resultant aerial distributions of amplitudes were plotted as colour displays, with variations in amplitude interpreted as representing depositional trends related to bulk lithological variations, with consideration for the effect of fluid fill on seismic amplitudes being made. The amplitude maps were then compared with facies data derived from cores and wireline logs, in order to ground-truth the lithological interpretations derived from the interpreted amplitude anomalies (Fig. 5). From this integrated data, a set of facies distribution maps for each fan and lobe were compiled. Biostratigraphical data was collected from all nine wells that intersected the Sea Lion Fan, the results of which are addressed in Holmes et al. (2015).

An acknowledgement is made that at the depth and scale of seismic resolution it is possible that a combination of seismic tuning effects (Simm and Bacon, 2014; Francis et al., 2015) and variations in fluid fill, may boost the observed amplitude anomalies. Thin bed tuning may be useful as it is controlled by variations in sedimentary body thickness, which is principally controlled by sedimentological processes. The seismic architectures observed in the amplitude extractions appear well-defined and are comparable in geometry to natural depositional features observed elsewhere (Adeogba et al., 2005; Fonnesu, 2003; Mayall et al., 2006 and 2010; Posamentier and Kolla, 2003; Prather et al., 1998a).

Turbidite Fans: The Sea Lion North, Sea Lion and Otter Fans

The turbidite fans within this study include: the Sea Lion North Fan, the Sea Lion Fan and the Otter Fan. The fans are represented by relatively subtle features on seismic sections, being characterised by both isolated and overlapping, relatively high-amplitude zones between continuous, lower amplitude seismic reflectors (Fig. 4). The Sea Lion Fan entered the basin from the Sea Lion feeder channel (Fig. 4). It is composed of three constituent lobes: Sea Lion 10, Sea Lion 15 and Sea Lion 20. The Sea Lion North Fan is younger than the Sea Lion Fan, entering the basin from a more-northerly located feeder channel, whilst the Otter Fan was likely penecontemporaneous with the deposition of the Sea Lion Fan, entering the basin from a more-southerly located feeder channel.

FACIES ANALYSIS

Twelve facies have been identified in the cores from the Sea Lion Fan (Table 1). These have been grouped into five facies associations representing similar depositional processes and settings (Fig. 6), which have been recognised in cores and interpreted in conjunction with a series of seismic amplitude maps (Fig. 7). These amplitude maps indicate the presence of features interpreted as lobe axis, lobe fringe and lobe distal fringe deposits, alongside other significant features and/or processes, including: feeder systems, flow deflection, flow constriction, sinuous lobe axis deposits, terminal mouth lobes and stranded lobe fringe areas.

The Lobe Axis facies association (Fig. 6i), the Lobe Fringe facies association (Fig. 6ii) and the Lobe Distal Fringe facies association (Fig. 6iii) can be used to characterise the three major elements of any lobe in the fan system, the terminology for which has been adopted from Prelat et al., (2009). The Hemi-Limnic Mudstones facies association (Fig. 6iv) represents the background sedimentation (suspension fall-out) within the lake. The Deformed Sandstones and Mudstones facies association (Fig. 6v) is interpreted as the product of dewatering or slumping of wet sediment immediately before or in-between periods of fan activity. In addition, Hybrid Event Beds are encountered in many of the cores (HEB; Fig. 6vi), typically found in combination with the Lobe Fringe facies association

Lobe Axis Facies Association

Description

This facies association (Fig. 6i) comprises fine to coarse grained, well to very well sorted, structureless sandstone (*fss*), parallel-laminated sandstone (*fpls*), mud-clast rich sandstone (*fmcs*), rafted mudstone clast-rich sandstone (*frms*) and graded structured sandstone (*fgss*; Table 1). The lobe axis facies association represents the dominant cored component within the Sea Lion Fan.

Up to 95% of the total thickness of each unit of the facies association is composed of beds of *fss* (Fig. 8a) which have sharp (non-erosional) contacts at the bed base (Figs 8b & 8c) and occasionally exhibit dish/dewatering structures (Fig. 8d). Beds dominated by *fss* sometimes exhibit normal grading, parallel laminations and an increase in the proportion of argillaceous material in the uppermost part of the bed. Successive beds

are mostly amalgamated but may be separated by an intervening mudstone. Individual beds range between 0.5 - 2 m in thickness and can be found in amalgamated packages reaching up to 15 m. In addition, there are common examples of 5-10 cm long, flattened, lithic-clast-armoured, angular mud clasts within facies mud-clast rich sandstone (*fmcs*, Table 1). These are typically concentrated in banded horizons in the middle or uppermost part of the beds dominated by *fss*.

Interpretation

The lobe axis facies association, represents deposition predominantly from high density turbidity currents in which high sediment concentration promoted deposition of structureless sandstone, dewatering and suppression of near-bed turbulence such that tractional sedimentary structures are subordinate. (Lowe, 1979; Haughton et al., 2009). The more fluidised versions of the flow, comprising dewatered, structureless sandstones (Fig. 6i) are not thought to be very effective at carrying sediment over long distances (Mutti, 1992). Amalgamated beds of *fss* along with the presence of *fmcs*, represents periods of erosion, indicating the presence of high energy flows operating in these locations.

The mud clasts present within these deposits were likely ripped-up and entrained in the flow from a location on the slope and were later deposited on the basin floor in a concentrated layer, forming at the boundary between a highly concentrated, non-turbulent carpet and an overlying turbulent layer (Postma et al., 1988). This transition marks the point where the buoyancy of the less-dense mud clasts and the flow velocity no longer supported their transport, resulting in deposition. The recognition of these features and their positioning within the bed is important as they indicate that at some point the flow was more erosional (Mutti & Nilsen, 1981; Haughton et al., 2003; Fonnesu et al., 2016).

Lobe Fringe Facies Association

Description

The lobe fringe facies association (Fig. 6ii) displays beds with more internal structuring including: very fine to fine grained, well sorted *fss*, ripple cross laminated sandstone (*frxls*), *fpls*, inter-bedded sandstone and mudstone (*fism*) and parallel-laminated mudstones (*fp/m*; Table 1). Beds tend to be significantly thinner (10 cm to 1

m), exhibit stronger normal grading, and have a greater thickness of structured sandstone facies (*frxls*, *fplm*) above the *fss* at the base of the bed compared to those of the lobe axis facies association. Beds are also less amalgamated and are thus often separated by 10-20 cm thick beds of *fplm*.

Interpretation

The increased occurrence of structures indicative of more dilute turbulent flow behaviour in the lobe fringe facies association, accompanied by the lowest occurrences of bed amalgamation (i.e. preservation of *fplm* and mudstone caps), thinner bedding, and finer grain size indicates a lower energy depositional environment located adjacent to the lobe axis. The upper-most, represented by *fism*, along with thickly bedded *fplm*, indicates periods of inactivity within the fan. In addition, a lack of evidence for channelization, in the form of inclined erosional surfaces or mud-clast rich, tractional lags at bed bases, helps support deposition within a lobe setting, opposed to a channelized setting.

Lobe fringe areas form a relatively low percentage of the aerial distribution within the Sea Lion Fan, especially compared to lobe axis deposits (Fig. 7). This is because the fans are relatively narrow, perhaps as a result of the constraints imposed by deposition within relatively narrow depressions formed adjacent to preceding deposits (partial confinement), and the fact that the branching, sand-rich systems therefore occupy much of the limited depositional space, preventing the widespread development of lobe fringe deposits. This narrowing of the facies belts along the elongated, partially confined lobes may result in abrupt facies variability internally within compensationally-stacked fan systems.

Lobe Distal Fringe Facies Association

Description

The lobe distal fringe facies association (Fig. 6iii) is characterised by a succession of thinly-bedded (10-50 cm), well sorted, very fine to fine grained, structureless sandstone (*fss*), followed vertically by well-developed ripple-cross laminated sandstones (*frxls*) and parallel-laminated mudstones (*fplm*) (Table 1; Fig. 8i). In general, mud clast are absent from this facies association. This facies association can be found in proximal, medial and distal parts of the Sea Lion Fan. The proximal version of the lobe distal fringe deposits are represented in core from well 14/10-5 in the Sea

Lion 10 lobe (Fig. 8i; Fig 11). The medial versions of the lobe distal fringe are observed in SL20 in well 14/10-6 (Fig 8iii; Fig.11) and are represented by a succession of *fss* and *frxls*, but with thicker interbeds of *fpls* and *fplm*. The presence of *fpls* and *fplm*, along with reduced bed amalgamation, provides a strong indication for a fringing location (Romans et al., 2009). To date, there is no core data from the distal versions of the lobe distal fringe facies of the Sea Lion Fan.

Interpretation

These deposits are interpreted to be the product of fully turbulent, low-density turbidity currents (Lowe, 1979; Haughton et al., 2009). They can be formed by the reduction of sediment concentration through prior deposition and flow run out into the lobe distal fringe locations. The presence of low-density turbidite structures in well sorted, very fine grained sandstones, in extremely proximal, lobe distal fringe locations indicates that flow transformation occurred abruptly, laterally away from the main depositional lobe axis, and not just through down-dip progression in the distal fan. This has led to vertical stacking of low-density turbidites. The thin-nature (1-2 cm) of capping beds of hemi-limnic mudstones (Fig. 8i) is interpreted to be a function of consistent activity of the adjacent lobe axis/lobe fringe setting and continued delivery of dilute(ed) turbidites into the lobe distal fringe areas, restricting the deposition of thickly-bedded hemi-limnic mudstones. Medial versions of the lobe distal fringe represent similar depositional processes, but contain more thickly developed, hemipelagic mudstones, representing longer breaks in sediment delivery to these locations, in comparison to the proximal locations.

For the Sea Lion Fan model, proximal and medial versions of the lobe distal fringe have been used as analogues for anticipated sedimentology found in the distal reaches of the fan. In the distal areas, more thinly bedded, finer grained versions of the lobe distal fringe are envisaged. These deposits are expected to contain thicker, more regular units of *fplm*, interspersed between the lower density turbidite deposits, representing periods of fan inactivity.

Hemi-Limnic Mudstones Facies Association

Description

The hemi-limnic mudstones facies association (Fig. 6iv) comprises 0.01-8 m thick units of *fplm* (Table 1.) They are inter-laminated with sparse, silt-grade laminae,

contain little evidence for bioturbation and otherwise are homogeneous except for occasional 1-8 cm thick, light grey to orange coloured, siliceous intervals of clay-grade material.

Interpretation

These deposits represent the background, hemi-limnic sedimentation of the lacustrine environment, with seasonal variations in productivity forming the laminations (Anderson and Dean, 1988). The light grey to orange coloured, siliceous intervals are interpreted as tonstein bands, deposited through volcanic ash-fall into a standing body of freshwater, typically described in coalfield successions (Spears, 2012).

As lacustrine deposition is relatively slow and constant, units of hemi-limnic mudstones can be used as an indication of the general activity or inactivity of each fan and lobe. In a very general sense, thin units of hemi-limnic mudstones represent breaks in turbidite deposition within one lobe, whereas significantly thicker units (perhaps >0.5 m) demonstrate major regional breaks in coarser-grained clastic deposition, potentially linked to fan de-activation and abandonment.

Deformed Sandstones and Mudstones Facies Association

Description

The deformed sandstones and mudstones facies association (Fig. 6v) represents packages comprised of well sorted, fine-grained sandstones, intercalated with siltstones and mudstones (Fig.10). They range from 0.05 to 3 m in thickness and are present as both relatively isolated occurrences or as thick intervals of disruption. Examples of deformed sandstones and mudstones can be found throughout the Sea Lion Fan, with the best examples observed in the Sea Lion 15 Lobe at the 14/10-7 well location (Fig. 7c).

Interpretation

The chaotic intercalation of sandstones and mudstones is interpreted to have been caused by a combination of: heavy dewatering; remobilisation of sandstones; and slumping or sliding. Features produced during dewatering include small mud/sand-volcanoes (Fig. 10a). In this example, primary fabrics have undergone a c. 90° rotation, indicating significant localised deformation and re-mobilisation. The arrangement of the facies makes it difficult to determine any defining facies evolution

or succession; much of the original, primary depositional structure has been disrupted. It is possible that some of the isolated occurrences (Fig. 10b) may represent the product of hybrid event beds formed by substrate de-lamination (Fonnesu, et al., 2016).

Hybrid Event Beds (mixed flow behaviour) – A Bed Type

Hybrid Event Beds represent the deposits of flows that exhibit mixed flow behaviour and are considered as a “bed type” in the model for the Sea Lion Fan. They are observed in association with lobe fringe deposition, but theoretically should also be found alongside lobe distal fringe deposits in the medial and distal parts of the fan (Davis et al., 2009). Unfortunately, the medial and distal expressions of the lobe distal fringe facies association are currently un-characterised in core data from the Sea Lion Fan.

Description

The hybrid event beds (Fig. 6vi) consist of a lower portion of *fss* overlain by a succession of argillaceous breccias (*fab1-3*; Table 1). Internally, the upper portion of the facies association is composed of three successive facies (*fab1-3*). These argillaceous facies typically exhibit sharp basal contacts, with the argillaceous matrix component of each successive facies increasing upwards above the sharp boundaries (Fig. 9). Facies *fab1* and *fab2* commonly display elongate, 1-5 cm long mud-clasts. In *fab3*, the larger mud-clasts have been replaced by a concentration of carbonaceous material in the matrix. These deposits are encountered in wells from the medial part of the Sea Lion Fan, in lobe fringe locations (SL15 in 14/10-6 and 14/10-7). In distal locations, they were not observed in the deposits of the lobe axis facies association (in 14/15-4Z) and there are currently no well penetrations through the lobe fringe or lobe distal fringe in this part of the fan.

Interpretation

This bed type represents the deposits of flows that exhibit evidence for mixed flow behaviour (Haughton et al., 2009 and Kane and Pontén, 2012). In the Sea Lion Fan, they have been observed in two examples from the SL15 lobe, in 14/10-6 and 14/10-7 (Fig 11.) In Haughton et al. (2009), these deposits are referred to as “hybrid event beds” and have been described in detail in, among many other examples, the deep-marine sediments of the North Sea (Barker et al., 2008; Davis et al., 2009; Haughton

et al., 2003; 2009); in the North Apennine Gottero Sandstone, north-west Italy (Fonnesu et al., 2015; 2017); the Springar Formation, Voring Basin, Norwegian North Sea (Southern et al., 2017); and the Marnoso Arenacea Formation, Italy (Amy and Talling, 2006).

The alternative model for the formation of hybrid beds, through relatively distal flow transformation, is presented in Kane et al., (2017). These have been referred to as transitional flow deposits in examples from the Gulf of Mexico (Kane and Pontén, 2012). The main difference between the two models is that the basal, structureless sandstone represents the product of distal flow collapse, as opposed to the product of a forerunning turbidity current (*sensu* Haughton et al., 2003; 2009). For the Sea Lion Fan, it is difficult to completely discount either model given the limited number of examples observed in core data, but we prefer to use the HEB terminology for the purposes of this study.

The basal unit of *fss* is interpreted to have been deposited rapidly, under a non-cohesive, high-density turbidity current and corresponds to “H1” in Haughton et al., (2009). The upper section, representing the *fab1-3* succession, was deposited under turbulence-suppressed, more cohesive conditions, facilitated by an argillaceous, finer grained component in the flow (Baas et al., 2009). The *fab1-3* sequence (Table 1; Fig. 9) represents the “debritic” portion of the hybrid event bed. These deposits are interpreted as hybrid event beds, which were the product of a single flow event undergoing flow-partitioning during downslope evolution, resulting in a flow which displays mixed behaviour (Haughton et al., 2003; 2009).

Internally, sharp jumps in argillaceous matrix content across the *fab1-3* boundaries are observed (Fig. 9). This may indicate further segregation or abrupt switches in flow rheology occurring within an already partitioned flow, alternatively these deposits could represent the product of transitional flows (Kane and Pontén, 2012). *Fab1* represents the lower most bed and can be equated to “H2” in Haughton et al. (2009), whereas the overlying *Fab2* can be equated to “H3”. The “H3” bed has since been further subdivided into six categories, termed “HEB 1-6” (Fonnesu et al., 2017). Lateral variability in H3 can be used to determine the processes which introduced fine grained material into the flow, whether it be up-dip turbulent erosion on the shelf; or substrate de-lamination in the basin (Fonnesu et al., 2016; 2017).

Fab3 is interpreted as representing the product of deposition out of suspension rather than forming part of the cohesive flow, with the loss of energy allowing the fine grained, light carbonaceous grains to settle and therefore concentrate. An alternative interpretation might be presented where the carbonaceous grains have been accumulated through longitudinal fractionation of the lighter components of the flow (Haughton et al., 2009). However, the relatively short transport distances in the Sea Lion Fan (5-10 km) may not permit efficient development of longitudinal segregation of fine-grained material. In some of the examples, *fab3* is absent (Fig. 9), which is probably a result of the original flow composition not containing much in the way of late-stage suspension material, resulting in poor preservation of this upper facies. The *fab3* facies is distinct from “normal” background settling as the water column has been disrupted and contains fines, such as carbonaceous material, that do not represent standard fall-out within the lacustrine environment.

SEISMIC AMPLITUDE ARCHITECTURES

Three sediment entry points, identified in 3D seismic data, along the eastern margin of the NFB are associated collectively with three fans, which can be subdivided into a total of six different individual lobes (Fig. 7). The “fan” and “lobe” nomenclature has been applied and refers to a single fan in which there are multiple lobes that are fed from one common, linked feeder system. Each of the three fans, and the lobes within the fans, display compensational-offset stacking (Fig. 4). Internally, within individual lobes, architectures are observed in seismic amplitude extraction maps (Fig. 7). The seismic amplitude architectures include: feeder systems, terminal mouth lobes, flow deflection, sinuous lobe axis deposits, flow constriction and stranded lobe fringe areas.

Feeder Systems

These features (Figs 7b, 7c & 7d) are observed as narrow (100 m – 300 m wide), downslope-widening, bright anomalies at the heads of fans and record the positions of sediment entry at the base of slope. The feeder systems appear to be detached from the up-slope areas, likely facilitated by slope bypass by the turbidite currents (Mutti et al., 1994, 2003; Stevenson et al., 2015). The detachment of the feeder systems from the slope margin is likely responsible for the successful up-dip stratigraphic sealing of the Sea Lion oil discovery.

Terminal Mouth Lobes

Terminal mouth lobe architectures (Figs 7b & 7d) are commonly observed in the medial-to-distal fan. These are represented in amplitude extraction maps as bright amplitudes with fanning-outwards geometries around 1.5 km in width. The well-defined, lateral limits of the bright amplitudes are coincident with the abrupt pinch-out of that seismic reflector (Fig. 7b). The terminal mouth lobes are dominated by stacked deposits of the lobe axis facies association. These are interpreted as the product of flows which may have bypassed the proximal-to-medial part of the fan, carrying coarse grained material into the distal part of the system. Bypass may have been enhanced by the partial confinement and elongation of the system, which acted to constrain the flow pathway, resulting in continuing delivery of fine-to-medium grained sand to the distally located terminal mouth lobes. The continuous delivery of sand to these locations is evidenced by bed amalgamation and the lack of development of intervening *fplm* in these locations (and dominance of lobe axis facies).

Flow Deflection

There are a few examples of flow deflection of one or more lobes by pre-existing palaeo-bathymetric highs. The highs are interpreted to be associated with earlier fan deposition, which may have acted to constrain the bed-to-lobe element scale (Prelat et al., 2009) fan and lobe deposits. Figure 7c illustrates the deflection of flows within the SL15 lobe by deposits of the older, pre-existing Sea Lion North fan (SLN). The similarity in size between each fan is an important factor to consider when examining flow deflection as this is likely to provide some control on whether flows surmount topography associated with the fan or are deflected by it.

Sinuuous Lobe Axis Deposits

Sinuuous lobe axis deposits are widely recognised on the amplitude maps from all of the fans and lobes (Fig. 7). They form very bright, high amplitude, relatively narrow features (approximately 100-1000 m wide) that extend basinwards for several kilometres. They are gently sinuous in nature and sometimes exhibit branching (Fig. 7d). The sinuous forms are oriented parallel to the main elongation axis of the fan, along the direction of flow from the confined feeder channels in the east, to the basin centre in the west. They have been cored in SL20 in 14/10-5 (Fig. 11) and are

dominated by less well sorted examples of the lobe axis facies association, which typically exhibit *frms*, particularly at bed tops.

Flow Constriction

Flow constriction of the lobe axis deposits has been observed, particularly in medial to distal locations (Fig. 7b). These features are interpreted to represent areas where the flow was being focussed, either as a result of passing between palaeo-bathymetric highs (e.g. Davis et al., 2009) or due to local increases in substrate gradient and subsequent incision of conduits that were eventually filled (Kneller, 2003). The flow constriction and down-flow branching may reflect flow transformation from high-density flow, to lower-concentration, less turbulent flows in the down-dip locations (Kneller, 2003). An alternative interpretation is possible, where such forms represent the neck of lobe deposits, which formed immediately down-dip from a zone of bypass across the fan surface (Fonnesu, 2003). In the Sea Lion Fan, there is no representative core through an area of flow constriction, limiting the interpretation of depositional processes at these sites.

Stranded Lobe Fringe Areas

Stranded lobe fringe areas, largely comprising deposits of the lobe fringe facies association, are recognised in all of the individual lobes comprising Sea Lion as relatively low amplitude zones separating sinuous lobe axis deposits (Fig. 7d). These are most pervasive in the medial parts of each fan. The stranded lobe fringe areas are distinct from surrounding mudstone dominated, basin-floor areas (e.g. outside the fan system).

DISCUSSION

Style, character and controls on deposition within the Sea Lion Fan

Seismic correlation and mapping of amplitude extractions and facies association distributions has facilitated the delineation of depositional facies zones across the Sea Lion 10, Sea Lion 15 and Sea Lion 20 lobes of the Sea Lion Fan (Figs 7 & 11). Each of the lobes has a proximal to distal elongated geometry, with lobe lengths approximately three times greater than their widths (13 km long vs. 4 km wide). The composite lobes are therefore relatively linear, and exhibit more restricted outwards spreading geometries than those observed in many deep-water marine systems

(Richards et al., 1998; Stow and Mayall, 2000; Mayall et al., 2006; 2010). The overall north-south elongated shape of the palaeo-bathymetry and the limited size of the basin is interpreted to have exerted some control on the axial nature of these features, with the fans flowing towards the deepest parts of the basin in the south.

The Sea Lion Fan accords with the “line-sourced, sand rich, slope apron fan” category of submarine fan types identified by Richards et al. (1998). Such features are usually small in terms of relative spatial distribution, have moderate to high slope gradients, a linear belt shape extending 1-10 km and a small, narrow shelf area. The high degree of sorting, as well as the presence of berthierine-coated grains (ooids) and pelletal glauconite within the turbidites have been used as evidence to suggest that they were fed from over-steepened, fringing lacustrine beach bars (Williams, 2015). These fringing beach bars may have been present along the basin margin (Figs 12 & 13), where the sediments were pre-sorted. The fringing shelfal clastics built up into beach deposits along the margin, until they became unstable and failed or were eroded into during episodic wetter periods (Fig. 14). This occurred at a number of different sediment feeder points located along the basin margin (e.g. Sea Lion North feeder, Sea Lion feeder and Otter feeder, Fig. 12).

Some of these feeder points supplied only one fan (the Sea Lion North Fan), whereas others were longer lived and were the site of multiple fan development (the Otter Fan and the Casper Fan, discussed in Bunt, 2015). Reasons why some fan feeders display relative longevity in terms of supplying multiple, temporally spaced fans to the basin whilst others supplied single fans are challenging to resolve with the existing data. One plausible explanation may be that river systems in the hinterland brought sediment into the fringing littoral system, which may have been re-worked and piled-up at specific locations, perhaps in areas where the shelf was slightly wider. This was then available to feed the deep-lacustrine fans through failure by over-steepening or re-working during down-cutting lowstand events. This re-use of sediment entry points, implies that basin-margin geometries and hinterland drainage systems may have exerted a large control on the loci of turbidite fan input along the eastern margin. At a regional scale, the Sea Lion Fan forms only one part of a series of southerly migrating fans arranged in a compensational-offset stacking pattern (Fig. 4). Input of sediment

was controlled by the southerly prograding delta that successively shut down these fans by choking the feeder systems (Fig. 14).

The triggering mechanism for the multi-phased delivery of sand into the NFB is still uncertain. Line-sourced, sand rich, slope apron fans tend to form predominantly during relative falls of base level, even though effective control of relative water level positions in terms of cycles and systems on the development or initiation of lacustrine fans is of low importance (Richards and Bowman, 1998). Many of the fans described above down-lap onto a regional unconformity surface (base of unit LC3 of Richards and Hillier, 2000a), which defines a significant hiatus in the southwards axial progradation of a major delta into the lacustrine basin during the early Cretaceous. Such relative falls of base level could have been triggered by faulting associated with regional uplift along the basin margin, causing lowering of the basin floor and sediment instability along the fringing shelf, resulting in the generation of the turbidite flows.

However, many of the fans within LC3 are underlain by at least one similar fan, developed below the LC3 unit's lower boundary as described in Lohr and Underhill (2015). These earlier fans have similar elongated, north-west/south-east oriented geometries to the fans within LC3. This implies that the mechanism controlling the origin and evolution of fans along the basin margin was operating prior to full-scale development of low-stand conditions in the basin coincident with major delta hiatus. Further discussion on the influence of basin margin geometries on sediment input along the eastern margin of the NFB can be found in Lohr and Underhill (2015). Fault geometry and activity at the basin margin is likely to have exerted a control on the position of the sediment entry points into the basin, providing discontinuities for the hinterland's drainage pathways (Lohr and Underhill, 2015). Richards et al. (2006) suggested that relay ramps along the basin margin may have provided sediment entry pathways for fan development into the basin. The Sea Lion Fan and Otter Fan feeders have similar orientations to the Sea Lion North Fan feeder channel, but display no corresponding evidence of underlying, controlling fault systems cross-cutting the basin margin fault. The point of maximum throw on the basin margin faults do not seem to coincide with the position of sand entry points along the margin. After entering the basin roughly perpendicular to the margin, the fans instead swing in a southerly direction, towards the basin's topographically lowest point (Fig. 12).

The role of partial confinement in controlling lacustrine systems

This study suggests that evidence for partial confinement of a system is presented by a combination of the following: sinuous lobe axis deposits, fan elongation, constriction of flow and flow deflection. The identification of elongated fans is important as it suggests that: flows were highly efficient, likely by virtue of high sediment volumes (Al Ja'aidi et al., 2004). The importance of recognising any form of confinement within a system, in this case partial confinement controlled by flow size and depositional topography, is that there may be potential for abrupt, lateral facies variability (as observed in Lomas and Joseph, 2004). When considering a compensationally stacked succession of turbidite fan and lobe deposits, the constraint of facies belts along elongated corridors through partial confinement may result in the aggradation of a highly complex suite of sediments.

There are a number of factors that may control partial confinement, including: the size of the flow and the amount of sediment entering the basin compared with the scale of the margin; the ability of deposits from preceding flows to control the next event bed pathway; factors that control flow efficiency, including flow volume and grain size distribution (Al' Jaidi et al., 2004); slope gradient; and a difference in flow rheology when sediment gravity flows enter a freshwater basin, compared with salt-water basins.

Effects of heterogeneity on hydrocarbon reservoir modelling

A consideration for the presence of heterogeneities within deep-lacustrine turbidite fans needs to be made, particularly in light of their increasing exploitation as hydrocarbon reservoirs. The identification of partial confinement within these systems suggests that lateral facies variability can be abrupt, facilitated by the elongation of the fans and constraint of facies belts. The vertical stacking of the lobes within the fans will lead to a complex facies model, with vertical stacking of highly variable sub-environments. This study also suggests that a "simple" proximal-to-distal degradation in reservoir properties will be insufficient for correctly modelling these systems.

One major aspect concerns the distribution of hybrid event beds, which are observed in association with lobe fringe deposition (Fig. 11) and the potential for enhanced development of these deposits in the lobe distal fringe. Most studies demonstrate that

hybrid event beds, deposited in deep-marine systems, are mainly present in the lobe fringe or more distal settings (Haughton et al., 2003; 2009; Talling, 2013; Kane et al., 2017). For example, hybrid event beds dominate the outer and distal parts of the Forties Fan of the Central North Sea, in the Everest, Lomond and Pierce fields (Davis, et al., 2009) and the Permian Skoorsteen Formation, in the Karoo Basin, South Africa (Hodgson, 2009). There are only rare examples where hybrid event beds are encountered in relation to channels (Terlaky and Arnott, 2014). Hybrid Event Bed deposits formed in lacustrine basins are rarely documented in the literature (another example being Tan et al., 2017).

Hybrid event beds contain elevated fines within the matrix, which greatly reduces poro-perm characteristics, commonly resulting in these units representing poor reservoir lithologies (Talling, 2013; Porten et al., 2016). An under appreciation for the distribution and thickness of these deposits will result in reduced oil reserves and, perhaps more importantly, these deposits have the potential to form baffles or barriers within the reservoirs (Amy et al., 2009).

Lacustrine Versus Marine Turbidite Systems

It is important to briefly highlight some of the similarities and differences between lacustrine systems and marine systems. Deep-water sedimentation in both marine and lacustrine settings appears to be composed of a similar suite of sediments, from high-density to low-density turbidite deposits, through to hybrid event beds and background, hemi-limnic deposition; the processes operating in the lacustrine environment are quite similar. The flows entering the basin form comparable depositional geometries, with fanning outwards of the systems and compensational stacking of internal lobes.

Some aspects of fan models developed in marine systems are clearly still applicable to deep-lacustrine basins. In particular, fan architectures of lacustrine turbidite systems, such as the Sea Lion Fan, may be more comparable to marine turbidite systems that are affected by confining palaeobathymetry (e.g. Lomas and Joseph, 2004; Amy et al., 2004). Lacustrine turbidite systems, deposited on an enclosed basin floor, are relatively small compared to that of the overall scale of the margin. Pre-existing palaeo-bathymetry will therefore be able to fundamentally affect the flow direction and impose a control over the velocity of the turbidite flows, which in-turn

may modify the resultant depositional geometries produced. The overall geometry of the basin has a strong influence on focussing the direction of any one, or a set of fan systems, towards the deepest parts of a lake. This is in contrast to an unconfined marine setting (Bouma et al., 2012), where lobe distribution remains relatively unrestricted. In these settings, the size of the fans entering the basin and the volume of sediment delivery are large, permitting the overriding of palaeobathymetry.

When turbidite fans in lacustrine basins are examined at the smaller scale of individual fans and lobes, feeder systems, sinuous lobe axis deposits and terminal mouth lobes can be identified. The main control over the constraint of the lobe axis deposits to sinuous belts is interpreted to be a function of the size of the flow entering the basin compared to pre-existing palaeobathymetry. Additionally, it is possible there is a critical difference between the rheology and characteristics of flows entering saltwater basins (marine) compared to flows entering basins filled with fresh-brackish water (lacustrine). The difference in fluid infilling these two types of basins may provide another important control on the partial confinement of the system, resulting in the architectural geometries observed in the Sea Lion Fan.

Ancient deep lacustrine turbidite fans are rarely described in the literature, making the Sea Lion Fan an important starting point in terms of research into deep-lacustrine fan systems. Given this, a number of major questions should be answered, these include: is there a difference in flow properties imparted by having a basin filled with fresh water as opposed to salt water?; Does this result in different styles of flow, where lobe axis deposits tend to follow more sinuous pathways?; Can this result in the ability of small variations in palaeo-bathymetry to impart enhanced control on flow direction? Future studies, such as outcrop studies and lab experiments (lock-gate), should focus on identifying differences between sediment gravity flows into fresh water and salt water basins.

CONCLUSIONS

1. Heterogeneity in lacustrine, partially confined turbidite fans can be modelled using a combination of amplitude maps, core data and wireline correlations.

2. Lacustrine fans can be relatively sand rich, but still contain numerous scales of heterogeneity, including both high and low-density turbidites, hybrid event beds and re-mobilised/deformed sediments.
3. Partial confinement of deep-lacustrine systems is evidenced by a combination of the following architectures: sinuous lobe axis deposits, fan elongation, constriction of flow and flow deflection.
4. The presence of hybrid event beds, along with other heterogeneities, have the potential to form complexity within lacustrine fan hydrocarbon reservoirs.
5. Deep-water marine and lacustrine environments display a set of sedimentary processes that form comparable deposits. However, observations of seismic architectures suggest that lacustrine systems may be more laterally constrained than compared with marine counterparts.
6. Lacustrine turbidite systems are likely more similar to confined marine systems than marine systems un-affected by confinement associated with seafloor topography.
7. Outcrop studies are required to characterize the sub-seismic aspects of lacustrine systems, which could be complemented by lab-testing in the form of lock-gate experiments, designed to examine differences in flow properties of sediment gravity flows into fresh versus salt water bodies.

ACKNOWLEDGEMENTS

Premier Oil and Rockhopper Exploration are thanked for kindly allowing the publication of commercial well-log, core and seismic data in advance of general public release. Premier Oil and Rockhopper Exploration stress that “the interpretations and opinions expressed in this paper are those of the authors and do not necessarily reflect the interpretations and opinions of the Sea Lion operator and partners.” We also thank staff from Desire Petroleum and Falklands Oil and Gas for their constructive comments on an earlier draft of this paper. Ian Andrews, Dave Schofield, Lucy Williams and Robert Newbould are specifically thanked for their helpful comments. Sarah Southern and Marco Fonnesu are thanked for their thoughtful and critical reviews that vastly improved the manuscript. Ian Kane and Nigel Mountney are thanked for editorial advice. The paper is published by permission of the Director, Mineral Resources, Falkland Islands Government, and the Executive Director, British Geological Survey (NERC).

REFERENCES

- Adeogba, A.A., McHargue, T.R. & Graham, S.A.** (2005) Transient fan architecture and depositional controls from near-surface 3-D seismic data, Niger Delta continental slope. *AAPG Bulletin*, 89, 5, 627-643.
- Al Ja'aidi, O.S., McCaffrey, W.D. & Kneller, B.C.** (2004) Factors influencing the deposit geometry of experimental turbidity currents: implication for sand-body architecture in confined basins. From: Lomas, S.A. & Joseph, P. (eds) (2004) *Confined Turbidite Systems. Geological Society, London, Special Publication*, 222, 45-58.
- Amy, L. A., McCaffrey, W. D., & Kneller, B. C.** (2004). The influence of a lateral basin-slope on the depositional patterns of natural and experimental turbidity currents. *Geological Society, London, Special Publications*, 221(1), 311-330.
- Amy, L.A. & Talling, P.J.** (2006) Anatomy of turbidites and linked debrites based on long distance (120-30km) bed correlation, Marnoso Arenacea Formation, Northern Apennines, Italy. *Sedimentology*, 53, 161-212.
- Amy, L.A., Peachey, S.A., Gardiner, A.A. & Talling, P.J.** (2009) Prediction of hydrocarbon recovery from turbidite sandstones with linked-debrite facies: Numerical flow simulation studies. *Marine and Petroleum Geology*, 26, 2032-2043.
- Anderson, R.Y. & Dean, W.E.** (1988) Lacustrine varve formation through time. *Palaeogeography, Palaeoclimatology, Palaeoecology*, 62, 215-235.
- Baas, J.H., Best, J.L., Peakall, J. & Wang, M.** (2009) A phase diagram for turbulent, transitional, and laminar clay suspension flows. *Journal of Sedimentary Research*, 79, 162-183.
- Barker, S.P., Haughton, P.D.W., McCaffrey, W.D., Archer, S.G. & Hakes, B.** (2008) Development of Rheological Heterogeneity in Clay-rich High Density Turbidity Currents: Aptian Britannia Sandstone Member, U.K. Continental Shelf. *Journal of Sedimentary Research*, 78, 45-68.
- Bouma, A. H., Normark, W. R., & Barnes, N. E.** (Eds.). (2012). *Submarine fans and related turbidite systems*. Springer Science & Business Media.
- Bunt, R.J.W.** (2015) The use of seismic attributes for fan and reservoir definition in the Sea Lion Field, North Falkland Basin. *Petroleum Geoscience*, 21, 137-149.
- Crossley, R.**, (1984) Controls on Sedimentation in the Malawi Rift Valley, Central Africa. *Sedimentary Geology*, 40, 33-50.
- Covault, J.A. & Romans, B.W.** (2009) Growth patterns of deep-sea fans revisited: Turbidite-system morphology in confined basins, examples from the California Borderland. *Marine Geology*, 265, 51-66.
- Davis, C., Haughton, P.D.W, McCaffrey, W., Scott, E., Hogg, N. & Kitching, D.** (2009) Character and distribution of hybrid sediment gravity flow deposits from the outer Forties Fan, Palaeocene Central North Sea, UKCS. *Marine and Petroleum Geology*, 26, 1919-1939.

Fonnesu, F. (2003) 3D seismic images of a low-sinuosity slope channel and related depositional lobe (West Africa deep-offshore). *Marine and Petroleum Geology*, 20, 615-629.

Fonnesu, M., Haughton, P.D.W., Felletti, F. & McCaffrey, W. (2015) Short length-scale variability of hybrid event beds and its applied significance. *Marine and Petroleum Geology*, 67, 583-603.

Fonnesu, M., Patacci, M., Haughton, P.D.W., Felletti, F. & McCaffrey, W.D. (2016) Hybrid Event Beds Generated By Local Substrate Delamination On A Confined-Basin Floor. *Journal of Sedimentary Research*, 86, 929-943.

Fonnesu, M., Felletti, F., Haughton, P.D.W., Patacci, M. & McCaffrey, W.D. (2017) Hybrid event bed character and distribution linked to turbidite system sub-environments: The North Apennine Gottero Sandstone (north-west Italy). *Sedimentology*, doi:10.1111/sed.12376

Francis, A., Lewis, M., & Booth, C. (2015) Sea Lion Field, North Falkland Basin: seismic inversion and quantitative interpretation. *Petroleum Geoscience*, 21, 151-169.

Fugitt, D. S., Stelting, C. E., Schweller, W. J., Florstedt, J. E., Herricks, G. J., & Wise, M. R. (2000). Production characteristics of sheet and channelized turbidite reservoirs, Garden Banks 191, Gulf of Mexico, USA. *The Leading Edge*, 19, 4, 356-369.

Griffiths, A. (2015) The reservoir characterization of the Sea Lion Field. *Petroleum Geoscience*, 21, 199-209.

Google Earth 7.1. (2017) 6°06'12.46S, 81°53'08.372W to 67°21'20.632S, 0°26'24.892E. US Dept of State Geographer Image Landsat / Copernicus, Data SIO, NOAA, U.S. Navy, NGA, GEBCO. Viewed 18/07/2017

Haughton, P.D.W., Barker, S.P. & McCaffrey, W.D. (2003). "Linked debrites in sand-rich turbidite systems – origin and significance. *Sedimentology*, 50, 459-482.

Haughton, P.D.W., Davis, C., McCaffrey, W.D. & Barker, S. (2009) Hybrid sediment gravity flow deposits – Classification, origin and significance. *Marine and Petroleum Geology*, 26, 1900-1918.

Hempton, M., Marhsall, J., Sadler, S., Hogg, N., Charles, R., & Harvey C. (2005) Turbidite reservoirs of the Sele Formation, Central North Sea: geological challenges for improving production. In: Dore, A.G. & Vining, B.A., (eds) *Petroleum Geology: North-West Europe and Global Perspectives – Proceedings of the 6th Petroleum Geology Conference*, 449-459.

Hodgson, D.M. (2009) Distribution and origin of hybrid beds in sand-rich submarine fans of the Tanqua depocentre, Karoo Basin, South Africa. *Marine and Petroleum Geology*, 26, 1940-1957.

Holmes, N., Atkin, D., Mahdi, S., & Ayress, M. (2015). Integrated biostratigraphy and chemical stratigraphy in the development of a reservoir-scale stratigraphic framework

for the Sea Lion Field area, North Falkland Basin. *Petroleum Geoscience*, 21(2-3), 171-182.

Jungslager, E.H.A. (1999) Petroleum habits of the Atlantic margin of South Africa. *In*: Cameron, N.R., Bate, R.H. & Clurie, V.S. (eds) *The Oil and Gas Habitats of the South Atlantic*. Geological Society, London, *Special Publications*, 153, 153-168.

Kane, I. A., Catterall, V., McCaffrey, W. D., & Martinsen, O. J. (2010). Submarine channel response to intrabasinal tectonics: The influence of lateral tilt. *AAPG bulletin*, 94(2), 189-219.

Kane, I.A. & Pontén, A.S.M. (2012) Submarine transitional flow deposits in the Paleogene Gulf of Mexico. Article in *Geology*, Nov 2012 DOI: 10.1130/G33410.1

Kane, I.A., Pontén, A.S.M. Vangdal, B., Eggenhuisen, J.T., Hodgson, D.M. & Spychala, Y. (2017) The stratigraphic record and processes of turbidity current transformation across deep-marine lobes. *Sedimentology*, 64, 1236-1273.

Kneller, B. (2003). The influence of flow parameters on turbidite slope channel architecture. *Marine and Petroleum Geology*, 20(6-8), 901-910.

Larsen, D. & Smith, G.A. (1999) Sublacustrine-fan deposition in the Oligocene Creede Formation, Colorado, U.S.A. *Journal of Sedimentary Research*, 69, 675-689.

Li, Q., Jiang, Z., Liu, K., Zhan, C. & You, X. (2014) Factors controlling reservoir properties and hydrocarbon accumulation of lacustrine deep-water turbidites in the Huimin Depression, Bohai Bay Basin, East China. *Marine and Petroleum Geology*, 57, 327-344.

Lohr, T. & Underhill, J.R. (2015) Role of rift transection and punctuated subsidence in the development of the North Falkland Basin. *Petroleum Geoscience*, 21, 85-110.

Lomas, S.A. & Joseph, P. (2004) Confined turbidite systems. *From*: Lomas, S.A. & Joseph P. (eds) (2004) Confined turbidite systems. *Geological Society, London, Special Publications*, 222, 1-7.

Lowe, D. R. (1979) Sediment Gravity Flows: Their Classification and Some Problems of Application to Natural Flows and Deposits. *SEPM Special Publication*, 27, 75-82.

Lyons, R.P., Scholz, C.A., Buoniconti, M.R. & Martin, M.R. (2011) Late Quaternary stratigraphic analysis of the Lake Malawi Rift, East Africa: An integration of drill-core and seismic-reflection data. *Journal of Palaeogeography, Palaeoclimatology, Palaeoecology*, 203, 20-72.

MacAulay F. (2015) Sea Lion Field discovery and appraisal: a turning point for the North Falkland Basin. *Petroleum Geoscience*, 21, 111-124.

MacDonald, D., Gomez-Perez, I., Franzese, J., Spalletti, L., Lawver, L., Gahagan, L., Dalziel, I., Thomas, C., Trewin, N., Hole, M. & Paton, M. (2003) Mesozoic break-up of SW Gondwana: implications for regional hydrocarbon potential of the southern South Atlantic. *Marine and Petroleum Geology*, 20, 287-308.

Mayall, M., Jones, E. & Casey, M. (2006) Turbidite channel reservoirs – Key elements in facies prediction and effective development. *Marine and Petroleum Geology*, 23, 821-841.

Mayall, M., Lonergan, L., Bowman, A., James, S., Mills, K., Primmer, T., Pope, D., Rogers, L. & Skeene, R. (2010) The response of turbidite slope channel to growth-induced seabed topography. *AAPG Bulletin*, 94, 7, 1011-1030.

Moernaut, J., Van Daele, M., Heirman, K., Fontijn, K., Strasser, M., Pino, M., Urrutia, R. & M. De Batist, (2014). Lacustrine turbidites as a tool for quantitative earthquake reconstruction: New evidence for variable rupture mode in south central Chile. *Journal of Geophysical Research: Solid Earth*, 119, 1607-1633.

Mutti, E. & Nilsen, T. (1981) Significance of intraformational rip-up clasts in deep-sea fan deposits. *Int. Assoc. Sedimentol. 2nd Eur. Regional Mtg. Abstr., Bologna*, pp. 117-119.

Mutti, E., & Normark, W. R. (1987). Comparing examples of modern and ancient turbidite systems: problems and concepts. In *Marine clastic sedimentology* (pp. 1-38). Springer, Dordrecht.

Mutti, E. (1992) (ed) *Turbidite Sandstones*. AGIP Istituto di geologia, Università di Parma, Italy, 275-276.

Mutti, E., Davoli, G., Mora, S. & Papani, L. (1994) Internal Stacking Patterns of Ancient Turbidite Systems from Collisional Basins. In: *Submarine fans and turbidite systems: Gulf Coast Section SEPM Proceedings, 15th Annual Research Conference*, 15, 257-268.

Mutti, E., Tinterri, R., Benevelli, G., Biase, D. & Cavanna, G. (2003) Deltaic, mixed and turbidite sedimentation of ancient foreland basins. *Marine and Petroleum Geology*, 20, 733-755.

Nelson, C.H., Karabanov, E.B., Colman, S.M. & Escutia, C. (1999) Tectonic and sediment supply control of deep rift lake turbidite system, Lake Baikal, Russia. *Geology*, 27, 163-166.

Porten, K.W., Kane, I.A., Warchol, M.J. & Southern, S.J. (2016) A sedimentological process-based approach to depositional reservoir quality of deep-marine sandstones: an example from the Springar Formation, north-western Vøring Basin, Norwegian Sea, *Journal of Sedimentary Research*, 86, 11, 1269-1286.

Posamentier, H.W. & Kolla, V. (2003) Seismic geomorphology and stratigraphy of depositional elements in deep-water settings. *Journal of Sedimentary Research*, 73, 3, 367-388.

Postma, G., Nemec, W. & Kleinspehn, K.L. (1988) Large floating clasts in turbidites: a mechanism for their emplacement. *Sedimentary Geology*, 58, 47-61.

Prelat, A., Flint, S. & Hodgson, D.M. (2009) Evolution, architecture and hierarchy of distributory deep-water deposits: a high-resolution outcrop investigation from the Permian Karoo Basin, South Africa. *Sedimentology*, 56, 2132-2154.

Prather, B.E., Booth, J.R., Steffens, G.S. & Craig, P.A. (1998a) Classification, Lithologic Calibration, and Stratigraphic Succession of Seismic Facies of Intraslope Basins, Deep-Water Gulf of Mexico. *AAPG Bulletin*, 82, 5A, 701-728.

Richards, M., Bowman, M. & Reading, H. (1998) Submarine-fan systems I: characterisation and stratigraphic prediction. *Marine and Petroleum Geology*, 15, 689-717.

Richards, M. & Bowman, M. (1998) Submarine fans and related depositional systems II: variability in reservoir architecture and wireline log character. *Marine and Petroleum Geology*, 15, 821-839.

Richards, P.C., Gatliff, R.W., Quinn, M.F. & Fannin, N.G.T. (1996a) Petroleum Potential of the Falkland Islands Offshore Area. *Journal of Petroleum Geology*, 19, 161-182.

Richards, P.C., Gatliff, R.W., Quinn, M.F., Williamson, J.P. & Fannin N.G.T. (1996b) The geological evolution of the Falkland Islands continental shelf. From: Storey, B.C., King, E.C., & Livermore, R.A., (eds), 1996 Weddel Sea Tectonics and Gondwana Break-up, *Geological Society Special Publication*, 108, 105-128.

Richards, P.C. & Fannin N.G.T. (1997) Geology of the North Falkland Basin. *Journal of Petroleum Geology*, 20, 165-183.

Richards, P.C. & Hillier, B.V. (2000a) Post-drilling Analysis of the North Falkland Basin – Part 1: Tectono-Stratigraphic Framework. *Journal of Petroleum Geology*, 23, 253-272.

Richards, P.C. & Hillier B.V. (2000b) Post-drilling Analysis of the North Falkland Basin – Part 2: The Petroleum System and Future Prospects. *Journal of Petroleum Geology*, 23, 273-292.

Richards, P.C., Duncan, I., Phipps, c., Pickering, G., Grzywacz, J., Hault, R. & Meritt, J. (2006) Exploring for Fan Delta Sandstones in the Offshore Falkland Islands. *Journal of Petroleum Geology*, 29, 199-214.

Romans, B.W., Hubbard, S.M. & Graham, S.A. (2009) Stratigraphic evolution of an outcropping continental slope system, Tres Pasos Formation at Cerro Divisadero, Chile. *Sedimentology*, 56, 737-764.

Ronghe, S. & Surarat, K. (2002) Acoustic impedance interpretation for sand distribution adjacent to a rift boundary fault, Suphan Buri basin, Thailand. *AAPG Bulletin*, 86, 10, 1753-177.

Saez, A. & Cabrera, L. (2002) Sedimentological and palaeohydrological responses to tectonics and climate in a small, closed, lacustrine system: Oligocene As Pontes Basin (Spain). *Sedimentology*, 49, 1073-1094.

Saller, A., Werner, K., Sugiaman, F., Cebastiant, A., May, R., Glen, D. & Barker, C. (2008) Characteristics of Pleistocene deep-water fan lobes and their application to an upper Miocene reservoir model, offshore East Kalimantan, Indonesia. *AAPG Bulletin*, Vol. 92, No. 7, pp. 919-949.

Scholz C.A., Rosendahl B.R. & Scott, D.L. (1990) Development of coarse-grained facies in lacustrine rift basins: Examples from East Africa, *Geology*, 18, 140-144.

Shanmugam, G., Shrivastava, S.K. & Bhagaban, D. (2009) Sandy debrites and tidalites of Pliocene reservoir sand in upper-slope canyon environments, offshore Krishna-Godavari Basin (India): Implications. *Journal of Sedimentary Research*, 79, 736-756.

Shanmugam, G. & Moiola, R.J. (1988) Submarine Fans: Characteristics, Models, Classification, and Reservoir Potential. *Earth Science Reviews*, 24, 383-428.

Simm, R. & Bacon, M. (2014) *Seismic Amplitude: An Interpreter's Handbook*. Cambridge University Press, ISBN 978-1-107-01150-2.

Smith, R.D.A. (1995) Reservoir architecture of syn-rift lacustrine turbidite systems, early Cretaceous, offshore South Gabon. *Geological Society, London, Special Publications*, 80, 197-210.

Southern, S. J., Mountney, N. P., & Pringle, J. K. (2014). The Carboniferous Southern Pennine Basin, UK. *Geology Today*, 30(2), 71-78.

Southern S.J., Patacci, M., Felletti, F. & McCaffrey W.D. (2015) Influence of flow containment and substrate entrainment upon sandy hybrid event beds containing co-genetic mud-clast-rich division. *Sedimentary Geology*, 321, 105-122.

Southern, S.J., Kane, I.A., Warchol, M.J., Porten, K.W. & McCaffrey, W.D. (2017) Hybrid event beds dominated by transitional-flow facies: character, distribution and significance in the Maastrichtian Springar Formation, north-west Voring Basin, Norwegian Sea. *Sedimentology*, 64, 747-776.

Spears, D.A. (2012) The origin of tonsteins, an overview, and links with seatearths, fireclays and fragmental clay rocks. *International Journal of Coal Geology*, 94, 22-31.

Stevenson, C.J., Jackson, C.A.L., Hodgson, D.M., Hubbard, S.M. & Eggenhuisen, J.T. (2015) Deep-Water Sediment Bypass. *Journal of Sedimentary Research*, 85, 1058-1081.

Stow, D. A., & Mayall, M. (2000). Deep-water sedimentary systems: new models for the 21st century. *Marine and Petroleum Geology*, 17(2), 125-135.

Straub, K. M., & Pyles, D. R. (2012). Quantifying the hierarchical organization of compensation in submarine fans using surface statistics. *Journal of Sedimentary Research*, 82(11), 889-898.

Talling, P.J. (2013) Hybrid submarine flows comprising turbidity current and cohesive debris flow: Deposits, theoretical and experimental analyses, and general models. *Geosphere*, 9, 3, 460-488.

Tan, M., Zhu, X., Geng, M., Zhu, S., & Liu, W. (2017). The occurrence and transformation of lacustrine sediment gravity flow related to depositional variation and paleoclimate in the Lower Cretaceous Prosopis Formation of the Bongor Basin, Chad. *Journal of African Earth Sciences*, 134, 134-148.

Terlaky, V. & Arnott, R.W.C.A. (2014) Matrix-rich and associated matrix-poor sandstones: Avulsion splays in slope and basin-floor strata. *Sedimentology*, 61, 1175-1197.

Williams, L.S. (2015) Sedimentology of the Lower Cretaceous reservoirs of the Sea Lion Field, North Falkland Basin. *Petroleum Geoscience*, 21, 183-198.

Williams, L.S. & Newbould, R. (2015). Introduction to the North Falkland Basin revisited: exploration and appraisal of the Sea Lion Field. *Petroleum Geoscience*, 21, 83-84.

Winker, C. D. (1996). High-resolution seismic stratigraphy of a late Pleistocene submarine fan ponded by salt-withdrawal mini-basins on the Gulf of Mexico continental slope. In Offshore Technology Conference. Offshore Technology Conference.

Zhang, S. (2004) The application of an integrated approach in exploration of lacustrine turbidites in Kiyang Sub-basin, Bohai Bay Basin, China. *Journal of Petroleum Science and Engineering*, 41, 67-77.

Zhi-qiang, F., Shun, Z., Cross, T.A., Zi-hui, F., Xi-nong, X., Bo, Z., Xiu-li, F. & Cheng-shan, W. (2010) Lacustrine turbidite channels and fans in the Mesozoic Songliao Basin, China. *Basin Research*, 22, 96-107.

Figure Captions

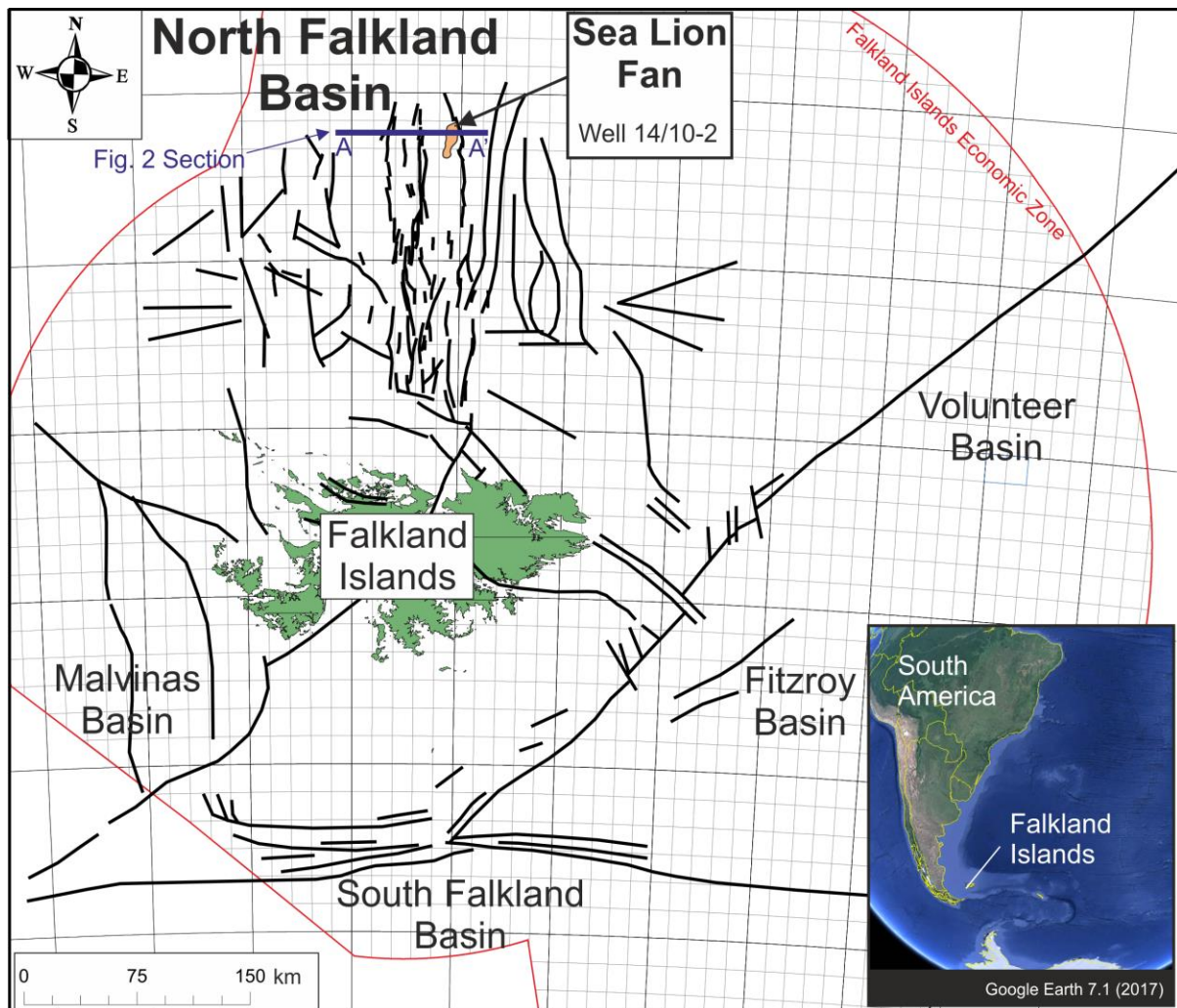


Figure 1. Map showing the location of the Falkland Islands located around 300 km to the southeast of South America (inset). The Falkland Islands are surrounded by several Mesozoic offshore basins including the NFB containing the Sea Lion Fan, which was deposited along one of the major north-south trending basin-bounding faults.

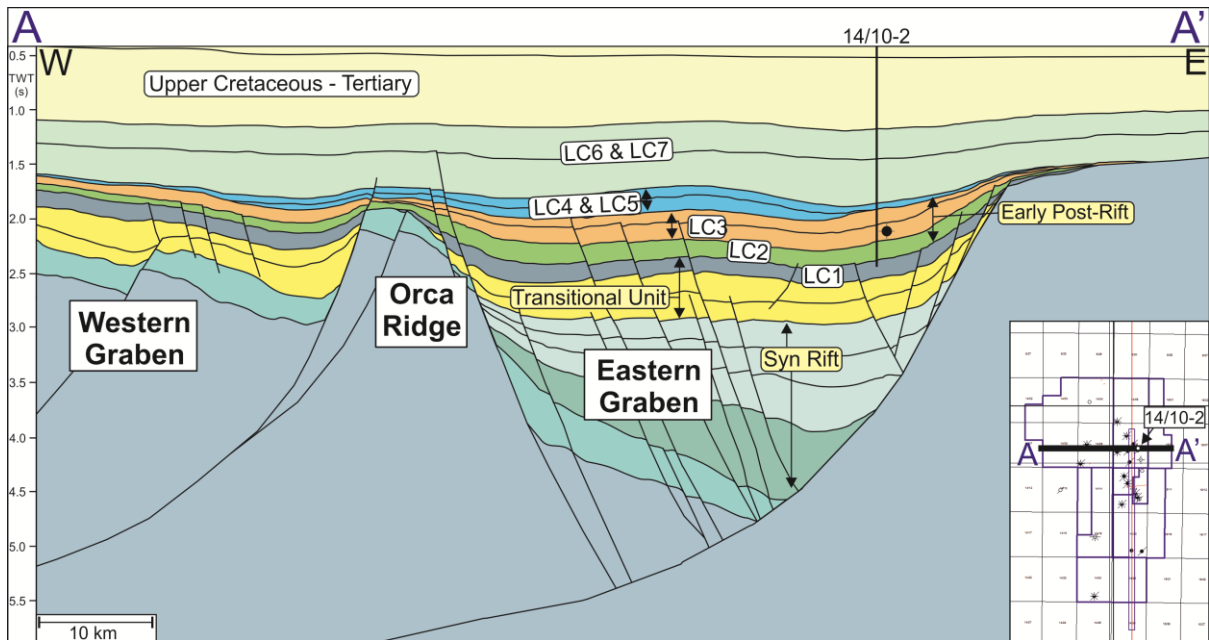


Figure 2. Line A-A' - Interpreted east-west orientated seismic line through the Sea Lion Fan of the NFB half-graben. The 14/10-2 Sea Lion discovery well encountered oil along the eastern flank of the NFB, in the LC3 tectono-stratigraphic unit, within the early post-rift basin fill.

| Period | Epoch | Age | Richards and Hillier, 2000a Tectono-Stratigraphy | | MacAulay, 2015 Stratigraphy | Eastern Margin Fans |
|------------|--------|-------------------------------|---|-------------|--------------------------------|--|
| Cretaceous | Lower | Aptian - Albian | Middle Post -Rift | LC7 | D4 - D9 | <div style="text-align: right;"> N S </div> |
| | | | | LC6 | | |
| | | Valanginian - early Aptian | Early Post-Rift | LC4 and LC5 | E1-E3 | |
| | | | | LC3 | F1 | |
| | | | | | F2 | |
| | | Berrassian- Valanginian | Transitional Unit | LC2 | F3 | |
| | | | | LC1 | | |
| ?Jurassic | ?Upper | Tithonian - Berrassian | Late Syn-Rift | "J2" | G1-2 | <div style="text-align: right;"> Casper Beverley Sea Lion Otter Sea Lion North </div> |

Figure 3. Stratigraphic column, displaying lithostratigraphical nomenclature for the NFB, modified after Richards and Hillier (2000a) and MacAulay (2015).

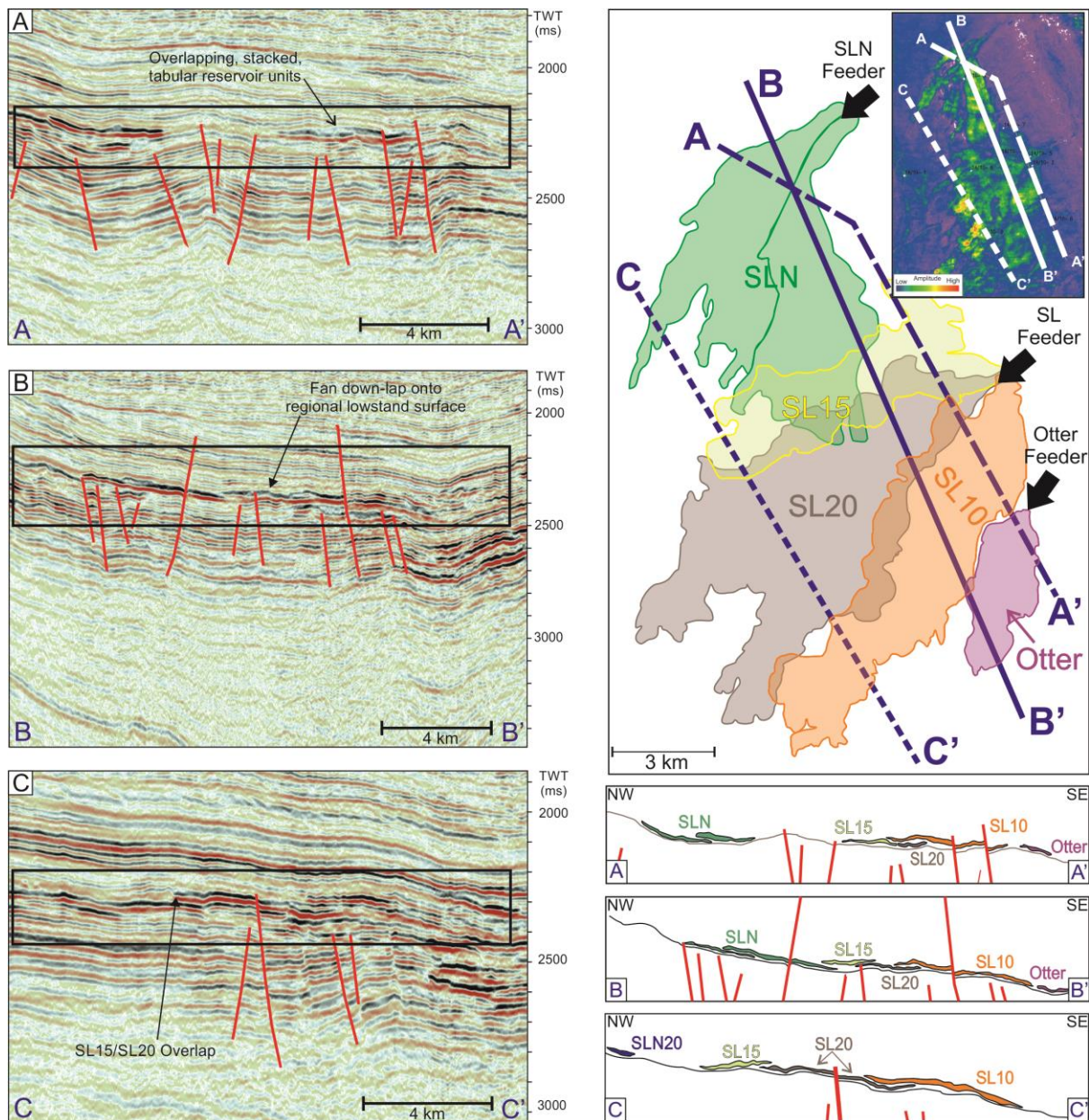


Figure 4. A series of full-stack, zero-phase, European polarity seismic and geoseismic sections, fan polygons and map illustrating the overlapping nature of the Sea Lion North Fan, Otter Fan and the Sea Lion Fan with composite lobes. **A.** Section A-A' illustrates the proximal setting, and shows the distribution of the overlapping tabular sands. **B.** Section B-B' illustrates the geometries of medial fan, characterised by overstepping, compensational stacking patterns. **C.** Section C-C' illustrates the distal overstepping geometries of the Sea Lion Fan lobes, more particularly how the SL15 lobe overlaps the SL20 lobe in the distal locations.

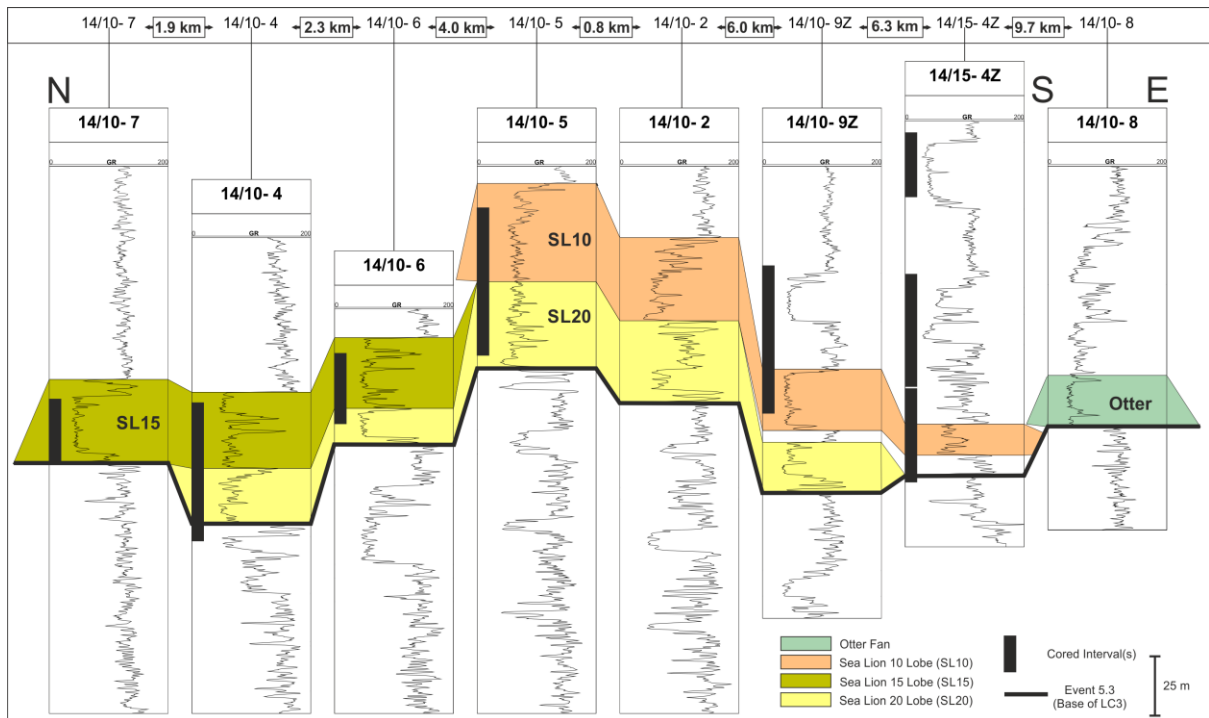


Figure 5. North-south-east orientated, correlated wireline logs (gamma-ray) hung on 2523.60 m (MD SSL). Moving from north-to-south, this correlation panel displays the SL15, SL20, SL10 lobes and the Otter Fan, which all rest on a lowstand surface, representing the base of LC3 (BGS seismic pick “event 5.3”). Correlations are based on seismic interpretation, in particular stacking geometries (indications for overlapping) and the determination of relative stacking patterns. The SL20 lobe represents the oldest deposits, which are overlain by the SL15 lobe and the SL10 lobe.

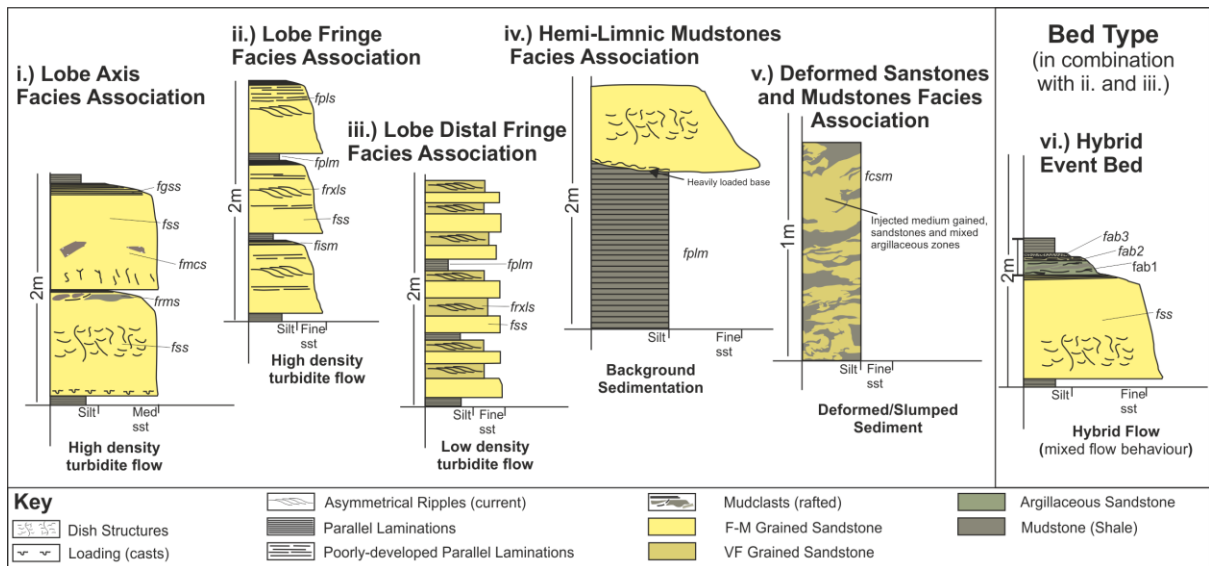


Figure 6. Idealised facies associations and bed types from cored sections of the Sea Lion Fan. The facies descriptions for the facies codes, referred to in this diagram, are contained within Table 1. **i.)** Lobe Axis facies association, **ii.)** Lobe Fringe facies association. **iii.)** Lobe Distal Fringe facies association. **iv.)** Hemi-Limnic Mudstones facies association **v.)** Deformed Sandstones and Mudstones facies association **vi.)** Hybrid Event Bed (bed type).

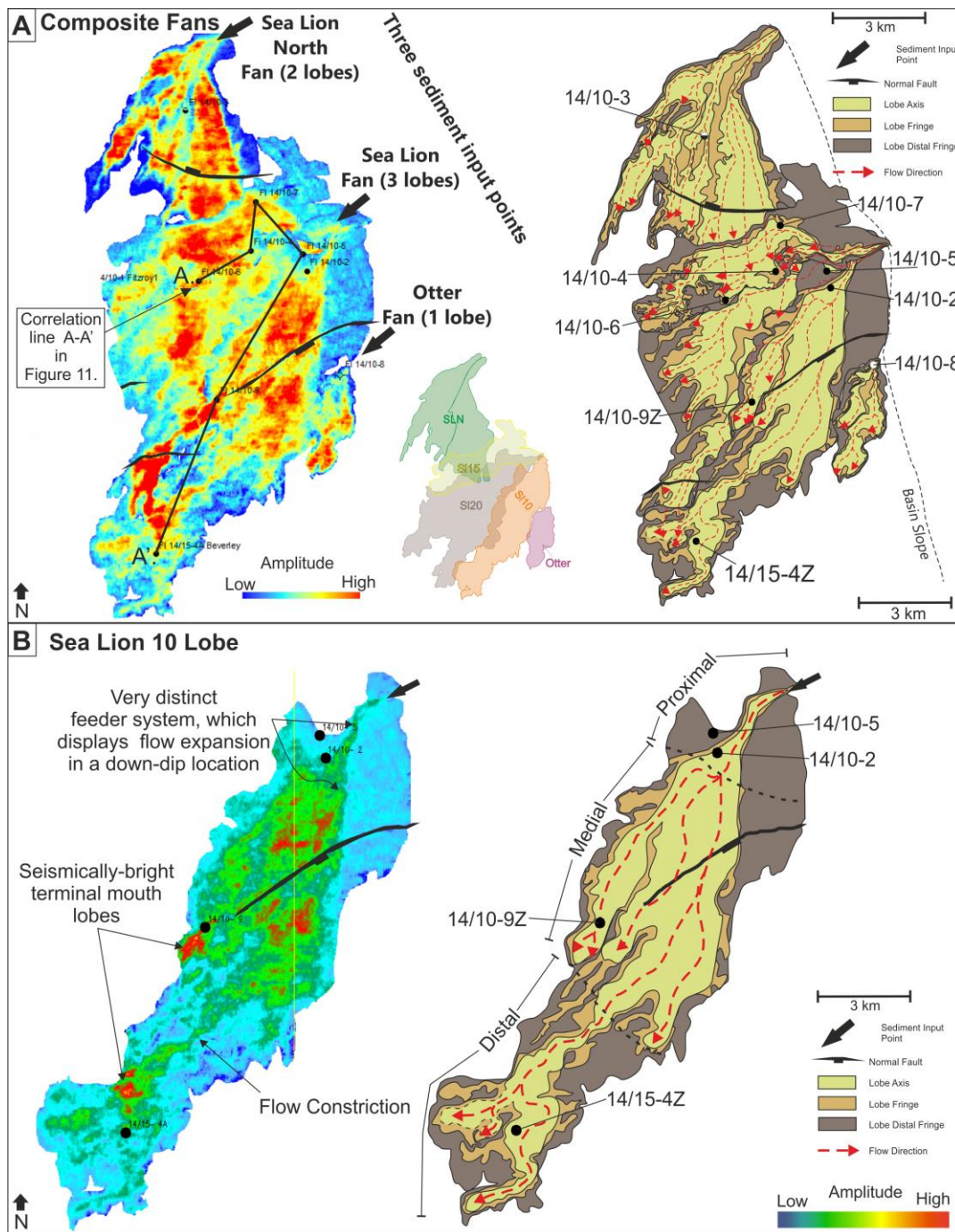


Figure 7. Interpreted seismic amplitude extraction maps of the Sea Lion North Fan, the Otter Fan and the Sea Lion Fan, displaying the Sea Lion Fan's component lobes: SL 10, SL 15, SL 20. Seismic amplitude extractions have been calculated from +/- 10 ms above a single, tabular seismic reflector. **A.** Composite map of three easterly derived fans, demonstrating the Sea Lion North Fan, the Sea Lion Fan's SL 10, SL 15, SL 20 lobes and the Otter Fan. The Sea Lion Fan comprises no less than three separate lobes, emanating from the same feeder position, located along the eastern flank of the NFB. **B.** The SL 10 lobe of the Sea Lion Fan.

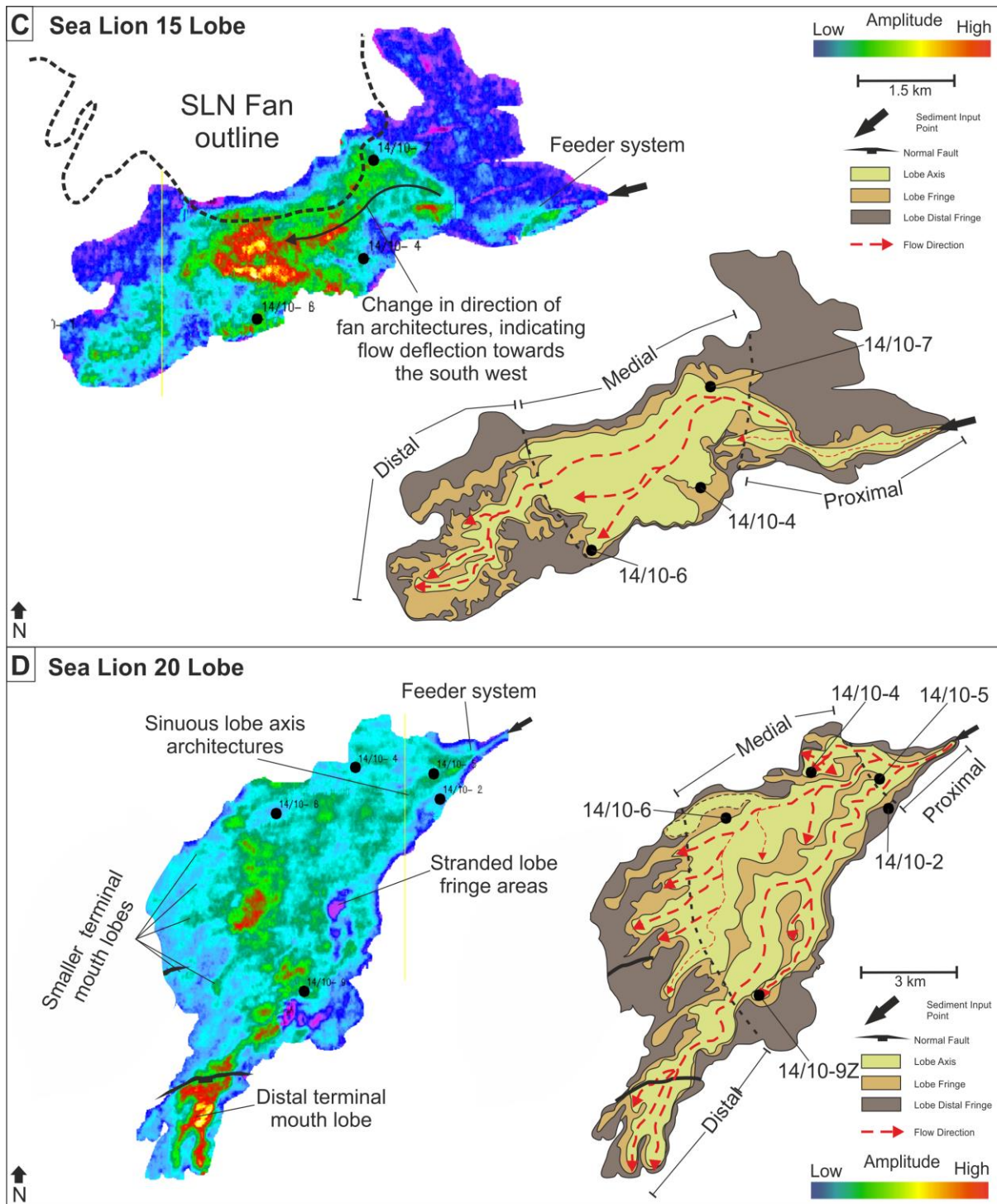


Figure 7C. The SL 15 lobe of the Sea Lion Fan. The distribution of the Sea Lion North Fan is marked by the dashed line, illustrating evidence for deflection of flow by pre-existing topography, formed by deposits of the older Sea Lion North Fan. **D.** The SL 20 lobe of the Sea Lion Fan.

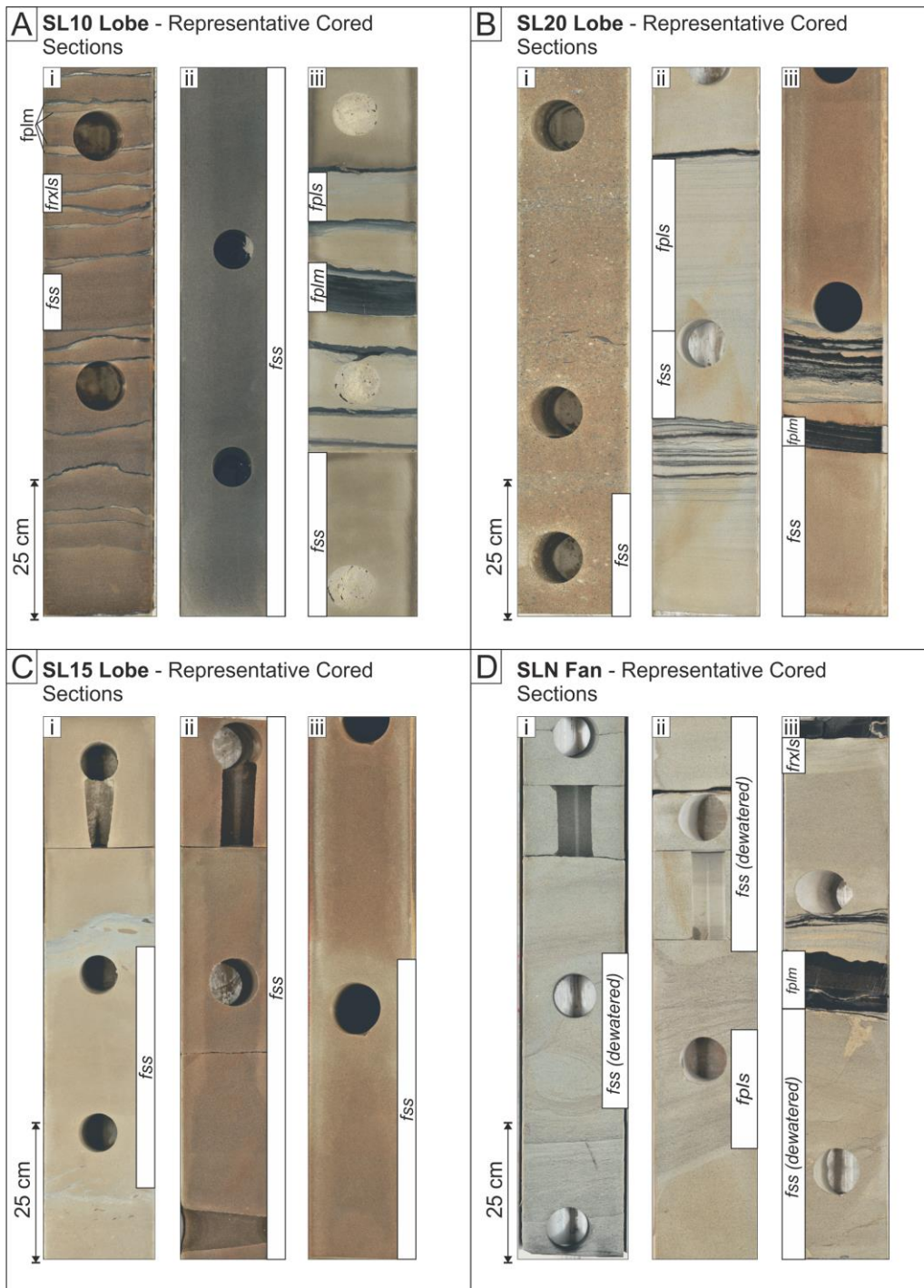


Figure 8. Representative core photography from the Sea Lion Fan illustrating the range and type of sedimentary features. **A.** Core from the SL10 lobe . **i.** *fss*, *frxls* and *fplm* observed in well 14/10-5. **ii.** *fss* **iii.** *fss*, *fpls* and *fplm*. **B.** Core from the SL20 lobe. **i.** *fss* **ii.** *fpls* and *fss* **iii.** *fss* and *fplm*. **C.** Core from the SL15 lobe. **i.** dewatered *fss* **ii.** *fpls* and *fss* **iii.** *fss*. **D.** Core from the Sea Lion North Fan **i.** dewatered *fss* **ii.** dewatered *fss* and *fpls* **iii.** dewatered *fss*, *fplm* and *frxls*.

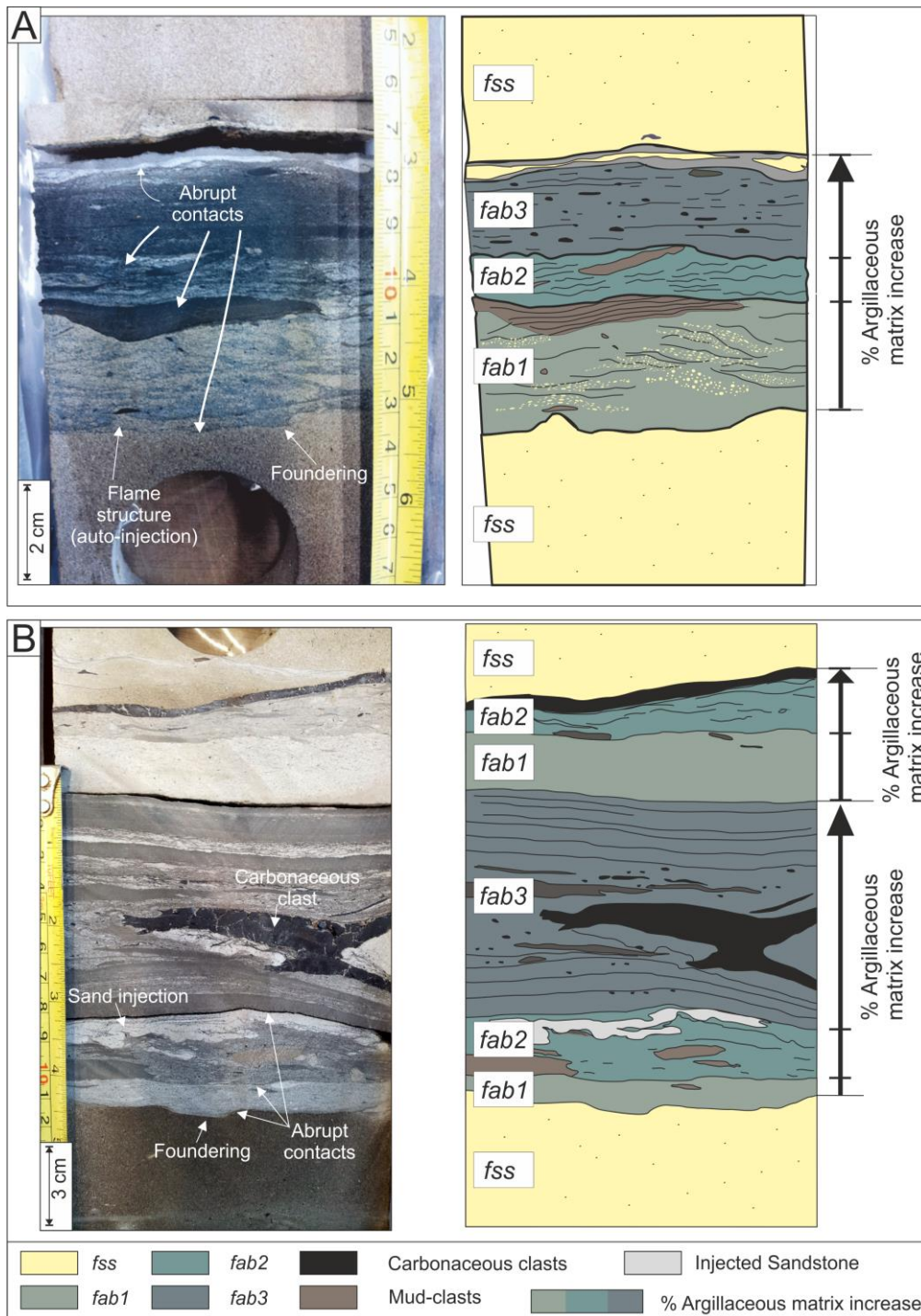


Figure 9. Examples of hybrid event beds from SL15, observed in wells 14/10-6 (2456.20 m) and 14/10-7 (2469.50 m). **A.** A hybrid event bed in 14/10-6, comprising the *fab1-3* facies succession and underlying structureless sandstone. **B.** Two stacked hybrid event beds in 14/10-7, with the upper-most facies, *fab3*, absent. In both examples, *fab2* contains a concentration of mudclasts. Instances of facies *fab3*, contain a concentration of carbonaceous clasts and smaller carbonaceous flecks in the matrices.

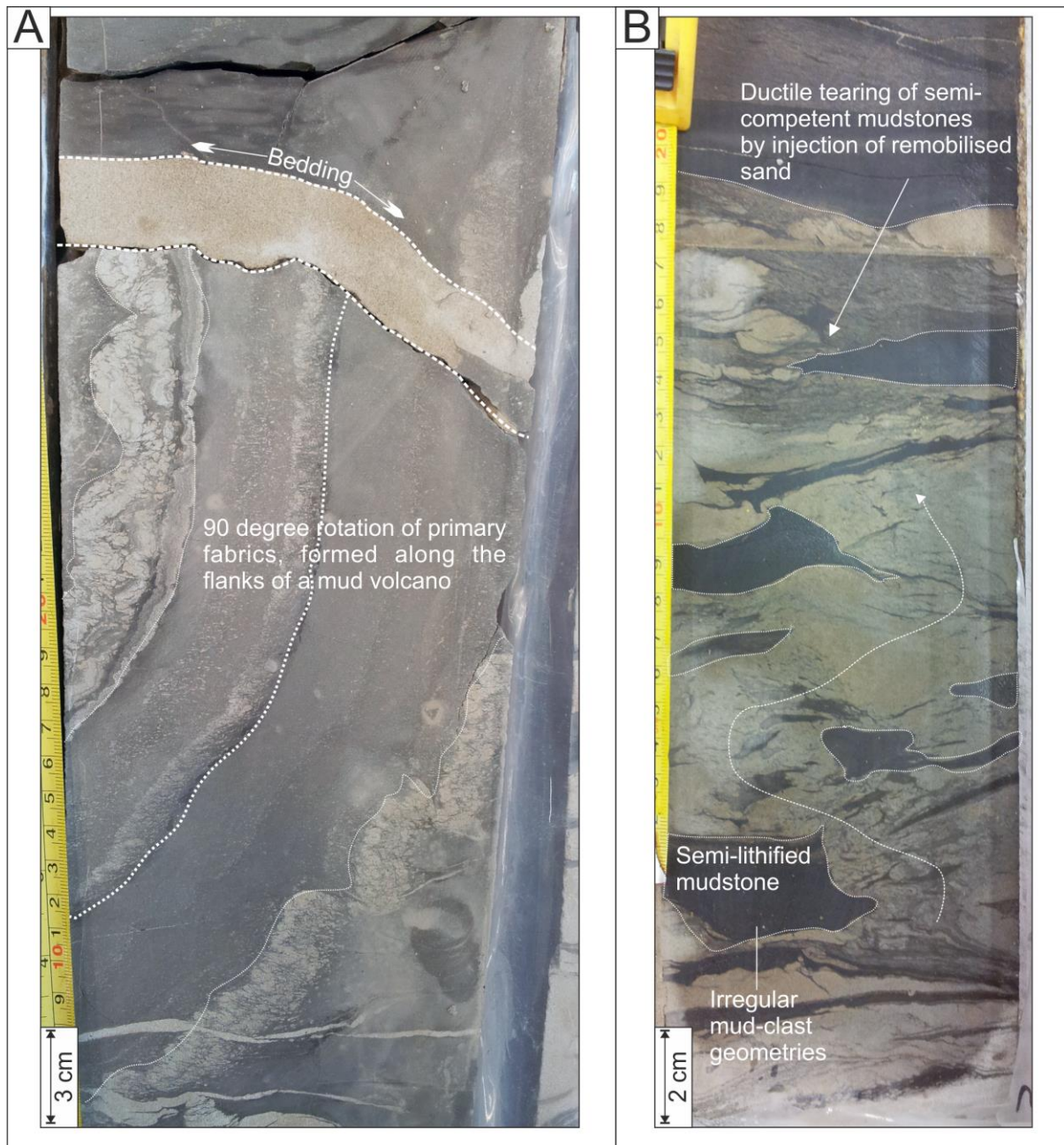


Figure 10. Examples of core photography from the Sea Lion Fan, displaying deformed sandstones and mudstones. **A.** A highly deformed, rotated, laminated unit that exists below a thick sandstone succession, interpreted as the flanks of a mud-volcano, which formed in response to dewatering of the lower beds by the imposing over-burden of the sandstones. **B.** Soft-sediment deformation, with tearing and stretching of more competent, yet ductile mudstone units by the injection of coarser-grained, fluidised material. This style of mudstone deformation suggests partial lithification of the mudstones prior to disruption.

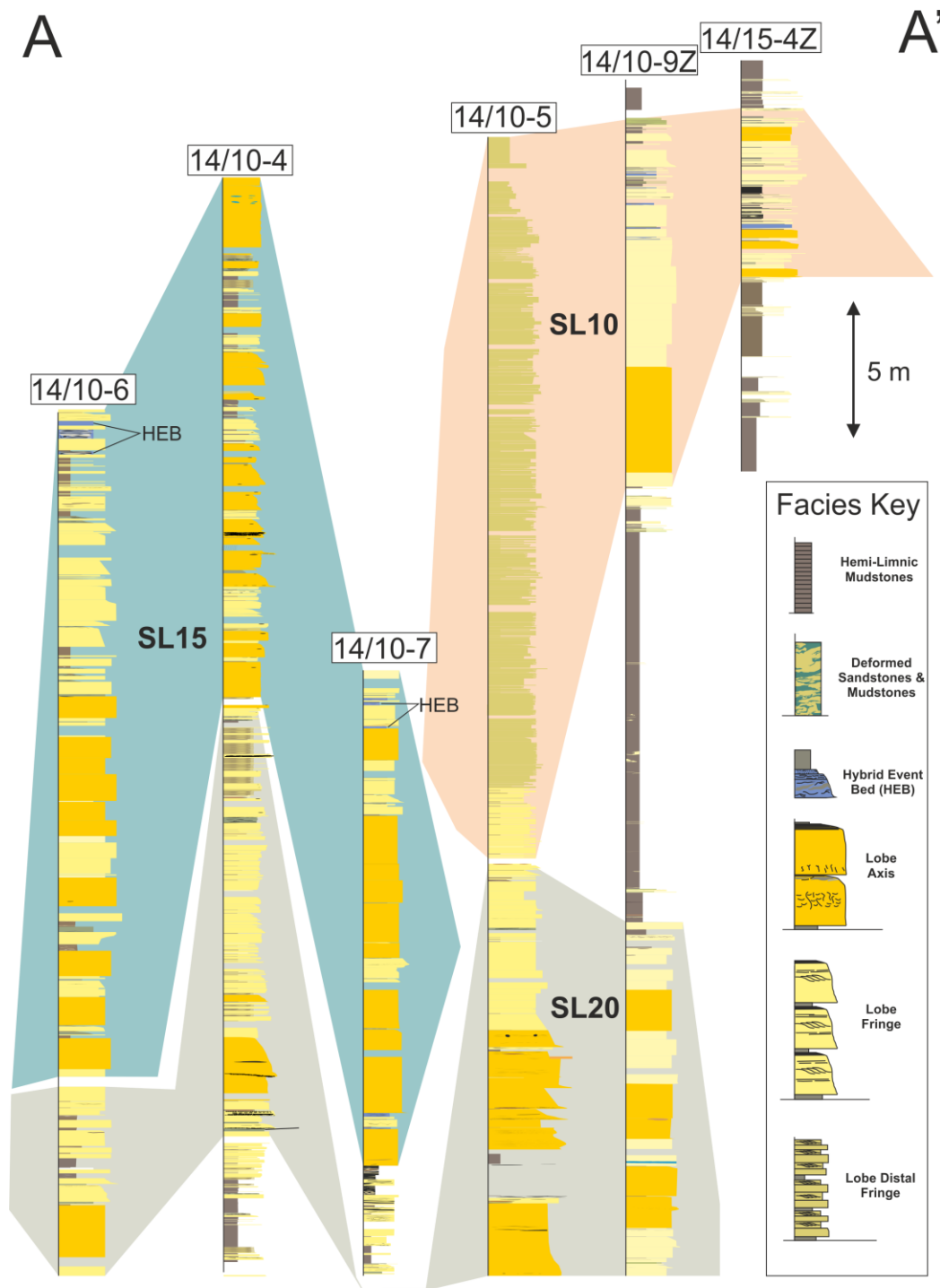


Figure 11. Correlated sedimentary core logs through the Sea Lion Fan (see Figure 7a. for the correlation map). The sedimentary logs have been colour-coded based on identified facies associations, which are illustrated in the facies key. Note the location of hybrid event beds in the SL15 lobe. Gaps in the logs represent preserved samples, which were unavailable for logging.

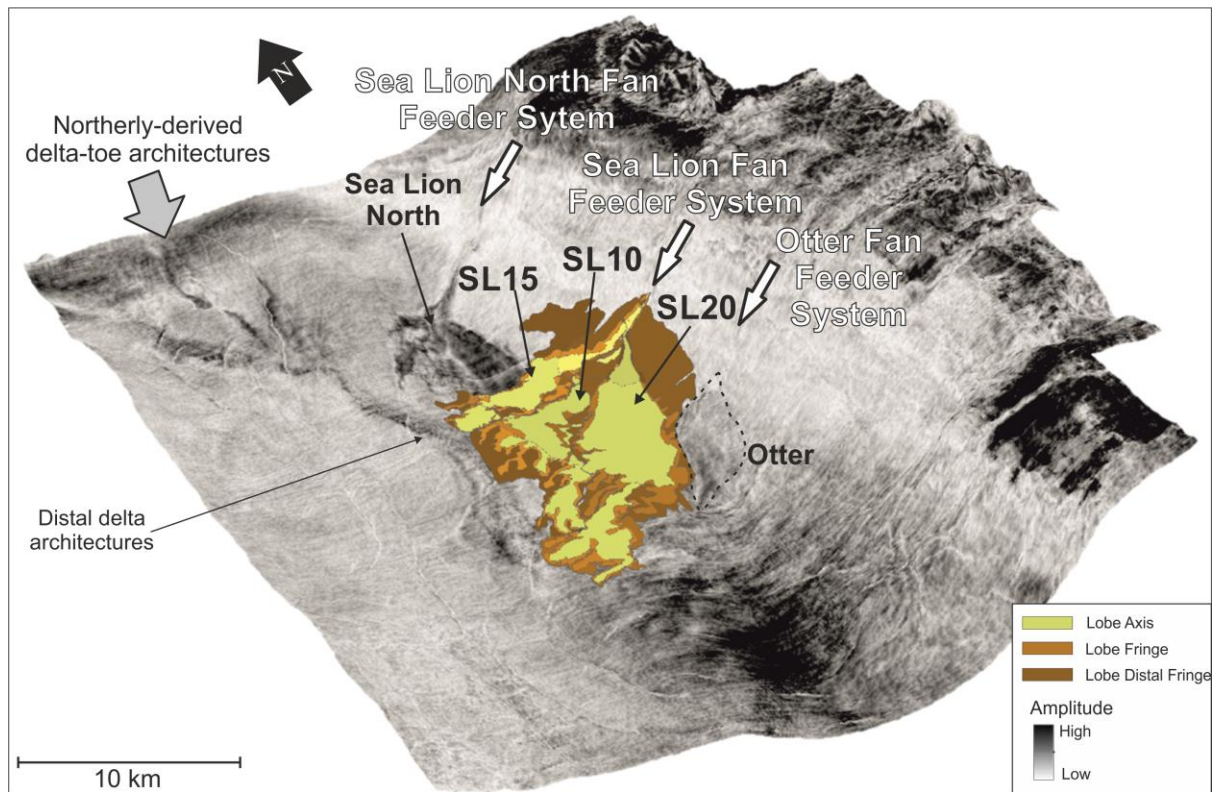


Figure 12. Three dimensional seismic amplitude surface showing: points of sediment entry into the basin; the location of the Sea Lion North and Sea Lion fans; and interpreted depositional facies for the Sea Lion Fan. The seismic surface comprises a 50 ms window of averaged seismic amplitudes from above the Valanginian-aged unconformity surface on to which the fans were deposited. The Sea Lion Fan was sourced from a feeder system located to the south of that which fed the Sea Lion North Fan. Distal delta-toe architectures, sourced from the north, inter-digitate with deposits of the Sea Lion Fan.

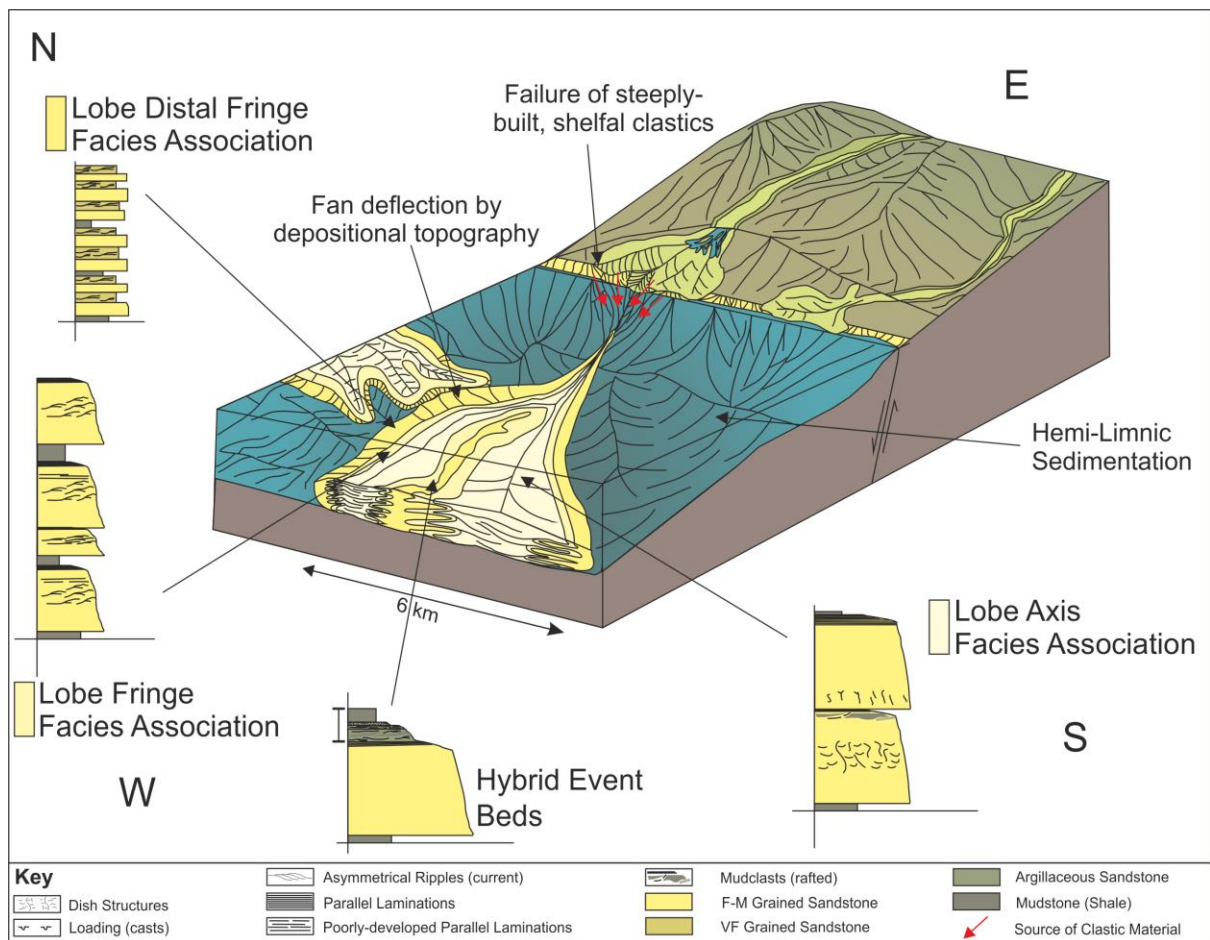


Figure 13. Schematic depositional model for the Sea Lion Fan, and more generally a model for deep-lacustrine turbidite deposition. Lobe axis deposits are located in the more axial positions and are represented by thick successions of stacked, amalgamated, high-density turbidites that comprise structureless sandstone. The lobe axis deposits are focussed along sinuous corridors, controlled by partial confinement. The lobe fringe deposits comprise high-density turbidites that are typically thinner and less-amalgamated with greater preservation of fine grained, parallel to current ripple laminated bed tops along with the presence of more regular, thicker-bedded hemi-limnic mudstones. Hybrid event beds are observed in lobe fringe depositional locations, associated with the isolated occurrences of structureless sandstone. Lobe distal fringe deposits are dominated by low-density turbidites that largely comprise parallel-laminated to ripple laminated sandstones and preservation of pervasive hemi-limnic mudstones.

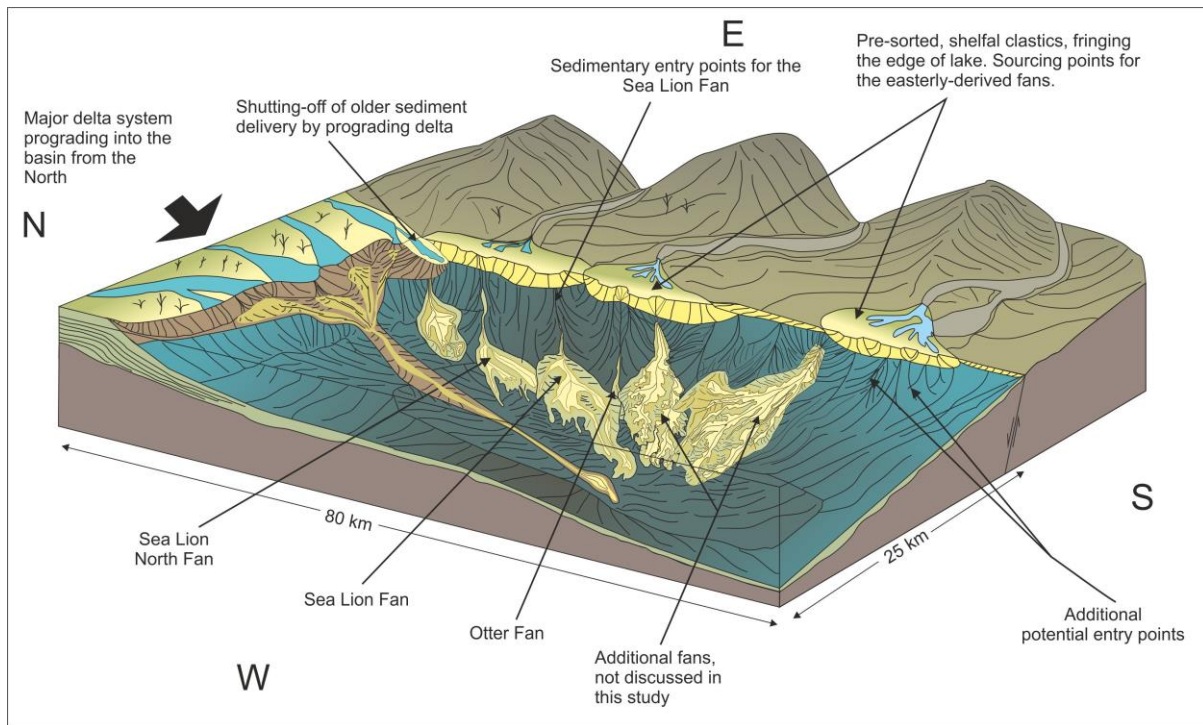


Figure 14. Schematic depositional environment for the NFB, during the Valanginian low-stand of the lake. A major axial delta prograded into the basin from the north, contemporaneously with the inclusion of the turbidite fans. These fans entered the basin from the eastern flank, forming sand-rich, slope apron features, draping the eastern basin slopes. Presence of detrital glauconite in these deposits suggests some element of pre-sorting in the shallow water environment, perhaps from a shelfal bar or fan delta. There is further evidence for Sea Lion-style fans, both geographically and stratigraphically throughout the NFB, indicating the potential for high sedimentation rates in the basin throughout the early Cretaceous.

Tables

Table 1). - Description and core photographs of sedimentary facies from the Sea Lion Fan

| Facies Code | Facies Title | Facies Descriptions | Interpretation | Example |
|--------------------|-------------------------------------|--|---|---|
| <i>frxls</i> | ripple cross laminated sandstone | Fine-to-medium grained, ripple cross laminated sandstone, with darker, sometimes carbonaceous/argillaceous silt-grade material, usually defining the ripple fore-sets. The thicknesses of this facies ranges from 2-10 cm, occasionally reaching 15 cm. | Current ripples formed through traction in a decelerating turbulent flow. |  |
| <i>fss</i> | structureless sandstone | Fine-to-coarse grained, well-sorted, sub-angular, quartz-dominated sandstone. Occasional dark coloured lithic grains and poorly developed argillaceous banding towards the top of the units. The facies comprises structureless sandstones with loaded bases, into underlying mudstones. Units of <i>fss</i> are found in stacked packages, up to 15 m in thickness, comprising up to 10 different amalgamated beds. | Rapid suspension fall-out from high density turbidite currents (Lowe 1982), with enhanced sorting controlled by extensive run-out distances. |  |
| <i>fgss</i> | graded structured sandstone | Medium-to-coarse grained, moderate-to-well sorted, sub-angular to sub-rounded sandstone displaying a coarse-grained base, normally grading to fine grained sandstone in the upper 2-3 cm of the bed. This facies typically comprises massive bedding and parallel laminations, which are particularly present in the upper portion of the bed. The top 2-3 cm contain elevated concentrations of clay-grade material. | Deposition in the tractional zone beneath a dilute turbulent flow (Allen, 1984) |  |
| <i>fplm</i> | parallel laminated mudstone | Dark grey to black coloured, homogeneous mud-to-silt grade, parallel laminated siliciclastic mudstones. The laminations are depicted by subtle variations in colour and grain size. This facies contains 3-10 cm wide, round siderite nodules that are scattered throughout. | Hemi-limnic suspension fall-out in the water column ("background sedimentation"). |  |
| <i>fmcs</i> | mudstone-clast rich sandstone | Fine-to-medium grained, well sorted, sub-angular, structureless sandstone that is mud-clast rich. This facies shares similar qualities to <i>fss</i> , with the addition of mud-clasts. Mud-clasts are elongated and range from 2 cm to 10 cm long, are sub-angular and are usually composed of mudstone or siltstone. They commonly display lithic grain armouring, indicating partial lithification prior to rip-up, entrainment and deposition. | Rapid suspension fall-out from high density turbidite currents (Lowe, 1982), with angular, armoured clasts indicating up-dip erosion (Haughton et al., 2003). |  |
| <i>fism</i> | inter-bedded sandstone and mudstone | Inter-bedded sandstones and mudstones. Sandstones are characterised as: very fine grained, ranging to medium grained, well sorted, sub-angular to sub rounded, structureless, occasionally parallel laminated and ripple cross bedded. Mudstones tend to be <1 cm-thick, homogenous and parallel laminated. Common examples of water escape structures and loading. Bioturbation is rare. | Post-depositional "re-working", slumping and churning through bottom-water processes and rare bioturbation. |  |

Table 1 cntd.) - Description and core photographs of sedimentary facies from the Sea Lion Fan

| Facies Code | Facies Title | Facies Descriptions | Interpretation | Example |
|-------------|---|--|--|--|
| <i>fpls</i> | parallel laminated sandstone | Very fine-to-medium grained, well sorted, sub-angular, parallel laminated, normally graded sandstone. The parallel laminations are sometimes highlighted by clay-to-silt grade material in the matrix. | Tractional laminations formed by a waning flow (Allen, 1984). |  |
| <i>fesm</i> | contorted (deformed) sandstone and mudstone | A chaotic assortment of mudstone and fine-to-coarse grained sandstone. Structuring includes: parallel laminations, dish structures, loading, ripple cross laminations particularly in the coarser sediments, along with common sections of poorly sorted, argillaceous-rich breccias. These units lack distinct boundaries and show complex geometries with over and underlying beds. | Slumping and re-mobilisation of soft sediments |  |
| <i>frms</i> | rafted mudstone clast-rich sandstone | Poorly sorted, fine-to-coarse grained, structureless, sub-angular, clast-rich sandstone. Clasts are composed of a mixture of rounded mud-clasts and sub-angular to sub-rounded lithic fragments. The mud-clasts tend to be suspended in the middle-to-upper portion of the bed and are fully-supported by the matrix. | Freezing of a high concentration flow, whilst in a laminar state (Mutti and Nilsen, 1981). High-density suspension of mud-clasts (Postma et al., 1988) |  |
| <i>fab3</i> | argillaceous breccia type 3 | Very fine grained, argillaceous-rich (approx. >25%), poorly-sorted sandstones and siltstones. This facies contains some examples of elongate, flattened mud-clasts and relative concentration of 1-5 mm wide carbonaceous material in the matrix. This facies displays poorly formed laminations along which some of the mud-clasts rest. | Suspension fall-out from a disrupted/perturbed water column. This could also be viewed as deposition through longitudinal fractionation of lighter components (Houghton, et al., 2009) |  |
| <i>fab2</i> | argillaceous breccia type 2 | Very fine grained, argillaceous-rich (approx. 15%), crudely laminated sandstone. There is a marked increase in argillaceous material within the matrix compared to that of in <i>fab1</i> . Commonly, this facies comprises 1-5 cm long, elongated and/or flattened mud-clasts along with poorly formed parallel laminations. | En masse deposition in a cohesive flow (Houghton et al., 2009). Crude parallel laminations may represent sheared sand patches (Fonnesu et al., 2017) | |
| <i>fab1</i> | argillaceous breccia type 1 | Very fine-to-fine grained, ripple laminated, poorly sorted sandstones, which display elevated argillaceous content (approx. 10%) within the matrix. There are common, 1-10 cm wide mud-clasts fragments within the matrix. Dewatering evidenced by dish structures has disrupted primary structuring, forming a chaotic "banding" of clean sandstone and light-grey coloured, clay-rich sandstone. | Transitional flow with intermittent turbulence suppression by dispersed argillaceous material (Houghton et al., 2009). | |